SIGMA-DELTA MODULATION BASED DISTRIBUTED DETECTION IN WIRELESS SENSOR NETWORKS

A Thesis

Submitted to the Graduate Faculty of the
Louisiana State University and
Agricultural and Mechanical College
in partial fulfillment of the
requirements for the degree of
Master of Science in Electrical Engineering

in

The Department of Electrical & Computer Engineering

by
Dimeng Wang
Bachelor of Engineering, Shanghai Jiaotong University, May 2005
August 2007

Acknowledgements

This thesis could not be finished without the help and support of many people who are gratefully acknowledged here.

First of all I would like to express my deepest gratitude to my advisors Dr. Shuangqing Wei and Dr. Guoxiang Gu for their consistent guidance and support to this thesis project, without which this work would not have been successful. All the valuable ideas and suggestions, as well as their patience and kindness are greatly appreciated. I have learnt from them a lot not only about doing academic research, but also the professional ethics. I am very much obliged to their efforts of helping me complete the thesis. I also wish to extend my thanks to Dr. Srivastava for being the member of my defence committee, and for his support of this thesis.

I would also like to thank my father Wencheng Wang and my mother Yanfei Yu for always being there for me. They never failed to give me great encouragement and confidence so that I can finish my study at LSU. Last but not least, I am also very grateful to all my friends in China and America. Special thanks should go to my girlfriend Yan Li for her support and help during my study, and making my life delightful.

Table of Contents

List of Figures

Abstract

We present a new scheme of distributed detection in sensor networks using Sigma-Delta ($\Sigma - \Delta$) modulation. In the existing works local sensor nodes either quantize the observation or directly scale the analog observation and then transmit the processed information independently over wireless channels to a fusion center. In this thesis we exploit the advantages of integrating $\Sigma - \Delta$ modulation as a local processor into sensor design and propose a novel mixing topology of parallel and serial configurations for distributed detection system, enabling each sensor to transmit binary information to the fusion center, while preserving the analog information through collaborative processing. We develop suboptimal fusion algorithms for the proposed system and provide both theoretical analysis and various simulation results to demonstrate the superiority of our proposed scheme in both AWGN and fading channels in terms of the resulting detection error probability by comparison with the existing approaches.

Chapter 1
Introduction

1.1 Distributed Detection

Distributed detection in wireless sensor networks has been gaining intensive research interests for decades. This interest was first sparkled by the requirement of military surveillance systems and has also been extended to other applications such as monitoring of environment since. In a distributed sensor network, multiple sensors work collaboratively to distinguish two or more hypothesis, e.g. tracking the presence of a phenomenon. Each local sensor performs some preliminary data processing and may send the information to other sensors. Ultimately the locally processed information is collected by a fusion center where a fusion decision is performed to reach a final decision based on the theory of statistical hypothesis testing.

Classical detection theory was first extended to the case of distributed sensors in [1] because of the consideration as cost, reliability, survivability, communication bandwidth in practical systems, applications and there is never total centralization of information where all the sensor signals are implicitly assumed to be available in one place for processing. There are three major topologies used in distributed signal processing: parallel, serial or tandem, and tree configuration [2, 3]. Parallel topology given in Fig. 1.1 is often adopted in recent research reports.

We will present a well accepted formulation of distributed detection problem. We assume a binary hypothesis testing problem in which the observations at all the sensors either correspond to the presence of a signal (hypothesis H_1) or to the absence of a phenomenon (hypothesis H_0). Suppose that there are N sensor nodes observing the random phenomenon and each sensor collects only one noisy observation. The observations $\{x_1, x_2, \cdots, x_N\}$

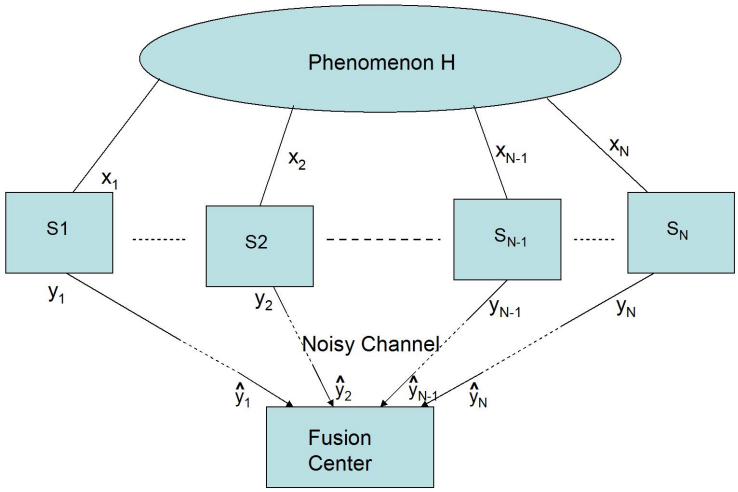

FIGURE 1.1. Distributed detection system scheme of parallel topology

at local sensors are characterized by the conditional probability density function (pdf) $f(x_1, x_2, \cdots, x_N|H_j), j = 0, 1$. Sensor nodes locally process the observation and transmit their outputs $\{y_1, y_2, \cdots, y_N\}$ to the fusion center over orthogonal wireless channels characterized by $f(\hat{y}_1, \hat{y}_2, \cdots, \hat{y}_N|y_1, y_2, \cdots, y_N)$.

The fusion center receives $\{\hat{y}_1, \hat{y}_2, \cdots, \hat{y}_N\}$ and makes a global decision θ based on an optimal or suboptimal fusion rule. Denote the prior probability by $\pi_j = P(H_j),\ j = 0, 1$. The detection performance is characterized by the detection error probability

$$P_{e,N} = \pi_0 P(\theta = H_1|H_0) + \pi_1 P(\theta = H_0|H_1) \tag{1.1}$$

The goal is to minimize the detection error probability by designing a proper local transmission strategy $\{\gamma_i\}_{i=1}^N$ that maps x_i to y_i and the corresponding fusion rule γ_0 that maps $\{\hat{y}_1, \hat{y}_2, \cdots, \hat{y}_N\}$ to θ at the fusion center. The optimal fusion rule at the fusion center is the maximum a posteriori probability (MAP) decision [4]

$$\gamma_0(\hat{y}_1, \cdots, \hat{y}_N) = \begin{cases} H_0,\ \Lambda \geq \frac{\pi_1}{\pi_0}, \\ H_1,\ \Lambda < \frac{\pi_1}{\pi_0}. \end{cases} \tag{1.2}$$

where

$$\Lambda = \frac{f(\hat{y}_1, \cdots, \hat{y}_N|H_0)}{f(\hat{y}_1, \cdots, \hat{y}_N|H_1)}$$

is the likelihood ratio (LR) of the joint probability density function (pdf) of $\{\hat{y}_i\}_{i=1}^N$ under each hypothesis.

In the context of data fusion, local decision strategy at each sensor node and global fusion rule at the fusion center should be dealt with in a collaborative manner to gain optimal system level performance. The situation becomes substantially more complicated when communication capabilities are integrated into each sensor and information may be lost in transmission. Binary sensor nodes which make binary decision locally were investigated earlier [5, 6, 1] and an universal detector has been constructed in [7]. Optimal local sensor detection does not necessarily yield a global optimal detection [1] and compromises should be made with each other as well as the fusion rule at the fusion center. Another type of sensor nodes adopts the local mapping strategy that directly retransmits the scaled version of the analog observation to the fusion center in order to preserve more information. Such sensor nodes will perform better with a high channel signal to noise ratio (SNR) [8]. Reference [6] shows that for the problem of detecting deterministic signals in additive Gaussian noise, having a set of identical binary sensor nodes is asymptotically optimal, as the number of observations per sensor goes to infinity. Thus, the gain offered by having more sensors exceeds the benefits of getting detailed information from each sensor as analog sensor nodes. However in practical systems, we will be more interested in the case that we have limited finite number of sensor nodes and observations. Indeed, there is a crossover between the two different mapping strategies dependent on different sensor and channel conditions [8].

Channel-aware distributed detection is proposed in [9, 10, 11] which integrates the wireless channel conditions in algorithm design. In [11], person by person optimization as well as greedy search methods are presented for optimal system detection performance. Fading channels receive more attention in recent research reports [12, 13]. Most design typically assumes the clair-voyant case, i.e. global channel state information (CSI) is known at the

design state In [12, 11], non-coherent detection where only channel fading statistics, instead of the instantaneous CSI are available to the fusion center. This is more practical since the exact knowledge of CSI may be costly to acquire. In the case of fast fading channels, the sensor decision rules need to be synchronously updated for different channel states. This adds considerable overhead which may not be affordable in resource constrained systems. Computational complexity is also an important issue because the optimal fusion rule such as likelihood ratio test (LRT) can be computationally very demanding even in synthesis of simple distributed detection networks [14]. Therefore, several suboptimal fusion rules are proposed and evaluated in [10]. The LRT based fusion rule reduces to a statistic in the form of an equal gain combiner (EGC) based on the assumption that all the sensors have the same detection performance and the same channel SNR.

Most of the research works mentioned above assume that sensor observations are conditionally independent (conditioned on the hypothesis), which implies that the joint density of the observations obeys

$$f(x_1, x_2, \cdots, x_N|H_j) = \prod_{i=1}^{N} f(x_i|H_j) \tag{1.3}$$

Although this assumption is easy to analyze, there are many occasions where the observations at the different sensors consist of noisy observations of random signals which were produced by the same source. General design principles are discussed in [15] for joint sensor detection of a deterministic signal in correlated noise. [16, 17] also explore the possibility of employing a shared multiple access channel (MAC) subject to an average power constraint instead of orthogonal parallel access channel (PAC). [18] focuses on such cases where sensor tests are based only on the ranks and signs of the observations, and non-Gaussian additive noise distribution is completely unknown. [19] provides two examples of detecting a constant signal in additive Gaussian noise and in Laplacian noise.

Generally there is no universal optimal distributed detection system scheme. Yet binary and analog sensor nodes with parallel configuration are the two prevailing strategies currently. Under the given framework their performance has crossover based on different channel and sensor observations. In this thesis we will develop a distributed detection scheme with a mixing topology of parallel and serial topologies which allow communication between adjacent sensor nodes. We will provide a local mapping strategy based on the well adopted Sigma-Delta ($\Sigma-\Delta$) modulation and a corresponding global LRT fusion algorithm at the fusion center.

1.2 $\Sigma - \Delta$ Modulation

Within the last several decades, the $\Sigma - \Delta$ modulation has become a popular technique for Analog to Digital converter (ADC) [20, 21]. It is a relatively simple yet challenging system because of its nonlinearity involved. The $\Sigma - \Delta$ converter digitizes an analog signal with a very low resolution (1 bit) ADC at a very high sampling rate. By using oversampling techniques in conjunction with noise shaping and digital filtering, it can achieve overall high resolution digital signal to reconstruct the analog signal.

Analog to digital Converter(ADC) is usually implemented in two separate processes: sampling and quantization. A continuous time signal is sampled at a uniformly spaced time intervals, T_s, the inverse of which is defined as the sampling rate. The sampling rate or sampling frequency f_s should be twice greater than the signal bandwidth f_B to avoid aliasing in signal spectrum that is known as the Nyquist Rate Conversion [22]. Once sampled, the signal samples must be then quantized in amplitude to a finite set of output values. An ADC or quantizer with L output levels is said to have M bits of resolution if $M = \lceil \log_2(L) \rceil$. It is obvious that the higher the resolution of an ADC has, the better performance it shall have in terms of the quantization error $e(n) = y(n) - x(n)$ and its

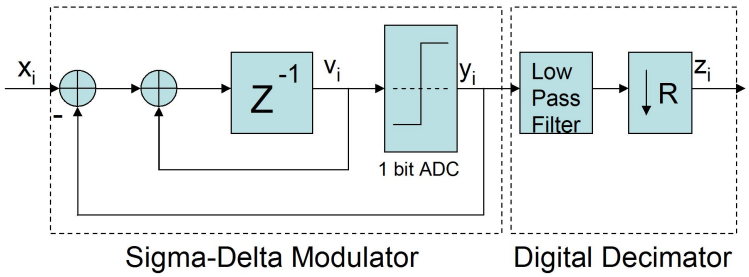

FIGURE 1.2. First order $\Sigma - \Delta$ modulator AD system

power $E(e(n)^2) = \sigma_e^2$ where $x(n)$ is the sampled input signal and $y(n)$ is its quantized version.

Consider an M bit ADC with $L_n = 2^M$ quantization levels and the maximum and minimum quantized outputs are always 1 and -1 respectively. The least significant bit (LSB) is defined as $\delta = 2/(L_n - 1) = 2/(2^M - 1)$. In practical systems, high resolution of a quantizer is usually not achievable due to the hardware complexity. Most conventional ADC, such as the successive approximation, subranging, and flash converters quantize signals sampled at or slight above the Nyquist rate. However, there are also other AD techniques such as $\Sigma - \Delta$ conversion that provide a tradeoff between resolution and bandwith by employing the oversampling technique, i.e., samples are acquired from the analog waveform at a rate significantly faster than the Nyquist rate. Each of these samples is quantized by an 1 bit ADC. The total amount of quantization noise power injected into the sampled signal σ_e^2 is exactly the same as the noise power produced by a Nyquist rate converter yet uniformly spread in the signal spectrum with a much higher sampling frequency f_s. After low-pass filtering and downsampling, which is known as the decimator, the quantization noise power is significantly reduced.

A block diagram of a first order $\Sigma - \Delta$ modulator A/D system is shown in Fig. 1.2. The modulator consists of and $\Sigma - \Delta$ modulator, followed by a digital decimator. The modulator consists of an integrator, an internal A/D converter or quantizer, and a feedback path.

The continuous-time signal is first oversampled before being input into the $\Sigma - \Delta$ modulator. The signal that is quantized is not the input $x(n)$ but the difference between the input and the analog representation of the quantized output and then pass through a discrete time integrator whose transfer function is $z^{-1}/(1 - z^{-1})$. Applying the linear model in [21], we obtain the Z domain relationship between the input and output of the $\Sigma - \Delta$ modulator,

$$Y(z) = X(z)z^{-1} + E(z)(1 - z^{-1}) \tag{1.4}$$

where $Y(z)$ and $X(Z)$ are the Z domain transform of input $x(n)$ and output $y(n)$ respectively. $E(Z)$ is the Z domain transform of the quantization noise $e(n) = x(n) - y(n)$. The output is now the input signal modulated by a signal transfer function $H_x(z) = z^{-1}$, plus the quantization noise modulated by a noise transfer function $H_e(z) = 1 - z^{-1}$, which is just a delayed version of the signal plus quantization noise that has been shaped by a first order differentiator or high-pass filter. To evaluate the performance of such a convertor, we need to find the total signal and noise power at the output of the converter. If a wide-sense stationary random process with power spectral density $P(f)$ is the input to a linear filter with transfer function $H(f)$, the power spectral density of the output random process is $P(f)|H(f)|^2$. Explicitly, signal power spectral density and noise power spectral density at the output of the $\Sigma - \Delta$ modulator are given as

$$P_{xy}(f) = P_x(f)|H_x(f)|^2 \tag{1.5}$$

$$P_{ey}(f) = P_e(f)|H_e(f)|^2 \tag{1.6}$$

where $P_e(f)$ is the power spectral density of the 1-bit quantizer error, which is white over the sampling frequency f_s and

$$P_e(f) = \frac{\sigma_e^2}{f_s}$$

where σ_e^2 is the quantization error power for a conventional Nyquist rate A/D converter. Assuming an ideal low-pass filter with cutoff frequency equal to the signal bandwidth f_B

following the $\Sigma - \Delta$ modulator, the in-band noise power, σ_{ey}^2 at the output of the A/D converter is

$$\sigma_{ey}^2 = \int_0^{f_B} P_{ey}(f)df = \int_0^{f_B} \frac{\sigma_e^2}{f_s}|H_e(f)|^2 df = \sigma_e^2 \frac{\pi^2}{3}(\frac{f_B}{f_s})^3 \tag{1.7}$$

Note that some of the noise power is now located outside of the signal band as the result of the oversampling. So the in-band power σ_{ey}^2 is less than what it would have been without any over sampling. Since the signal power is assumed to occur over the signal band only, it is not modified in any way and the signal power at the output σ_{xy}^2 is the same as the input signal power σ_x^2. This oversampling process reduces the quantization noise power in the signal band by spreading a fixed quantization noise power over a bandwidth much larger than the signal band. On the other hand the noise transfer function modulates the quantization noise spectrum by further attenuating the noise in the signal band and amplifies it outside the signal band. Consequently, this process of noise shaping by the $\Sigma-\Delta$ modulator can be viewed as pushing quantization noise power from the signal band to other frequencies. The modulator output can then be low-pass filtered to attenuate the out of band quantization noise and finally can be downsampled to the Nyquist rate. The output of the digital decimator thus becomes a multi-bit finite-valued digital data reconstructing the analog input.

The linear model in (1.4) is rather an approximation due to the nature of nonlinearity involved in $\Sigma - \Delta$ modulation. [23, 24] investigate the statistic characteristics of $\Sigma - \Delta$ modulation with independent identical distributed (i.i.d) Gaussian input which provide us more insight of its time domain behavior. Preliminary research reports also propose schemes that integrate $\Sigma - \Delta$ data converter into wireless transceiver [25, 26]. [27] presents a radio frequency identification (RFID) temperature sensor design embedded with $\Sigma - \Delta$ ADC. An iterative computation process to obtain the joint pdf of $\Sigma - \Delta$ outputs is studied in [26].

1.3 Contribution

In this thesis, we propose a novel distributed detection scheme for binary hypothesis test. We are motivated by the fact that analog mapping strategy preserves more information regarding the hypothesis while binary transmission is robust against wireless channel distortion. Inspired by the concept of analog to digital converter which converts analog signals to bit-stream, we propose a novel $\Sigma - \Delta$ modulation-based distributed detection scheme where wireless sensor nodes jointly process the analog observations using $\Sigma - \Delta$ modulation without oversampling and decimation. Due to the limited power budgets, each local sensor is only allowed to take one sample of observation and send one bit message to the fusion center. Furthermore, each sensor is allowed to communicate to its next adjacent sensor, considering that the communication over the wireless channel between the two adjacent sensors is more reliable than the channels between sensors and the fusion center. The novel combination of serial and parallel topology enables us to form an equivalent $\Sigma - \Delta$ loop across space within the wireless sensor network. As shown in our simulation results, the $\Sigma - \Delta$ modulation-based distributed detection system outperforms both the binary and analog approaches in both AWGN channels and fading channels under certain conditions.

Our thesis is organized as follows. Motivating examples of single sensor detection using $\Sigma - \Delta$ modulation are first presented in Chapter 2. Distributed detection in AWGN channels is studied in Chapter 3. The $\Sigma - \Delta$ modulation-based distributed detection system is formulated in Section 3.1. Suboptimal fusion rule as well as analytical detection performance of $\Sigma - \Delta$ modulation based distributed detection system in AWGN channels are derived in Section 3.2. LRT-based fusion rules of binary and analog distributed detection system are presented in Section 3.3. Detection performance evaluation is provided in Section 3.4. We investigate the system over non-coherent fading channels in Chapter 4. An iterative computation process to obtain the joint pdf of the $\Sigma - \Delta$ modulator output is presented in Section 4.2. We develop the LRT-based fusion algorithm for $\Sigma - \Delta$ modula-

tion based distributed detection system in Section 4.3. Optimal fusion rules of binary and analog distributed detection system in fading channels are presented in Section 4.4. Similarly detection performance in fading channels is evaluated via simulations in Section 4.5. Extensive study on distributed detection over coherent fading channels and of correlated observations is presented in Chapter 5. Finally, the thesis is concluded in Chapter 6.

Summary

In this chapter, we

- Introduce the distributed detection system and review the related works.
- Introduce the $\Sigma - \Delta$ modulation AD converter and review its applications in wireless communication.

Chapter 2

Single sensor detection using $\Sigma - \Delta$ Modulation

Before we exploit the distributed sensor detection using $\Sigma - \Delta$ modulation, in this chapter we will first provide a motivating example to demonstrate how to integrate $\Sigma - \Delta$ Modulator into single sensor design for detection with multiple input. With rigorous analysis to be presented in the next two chapters, we will observe the robust performance of $\Sigma - \Delta$ Modulation based detection via a sequence of simulations.

2.1 Sensor node embedded with a first order $\Sigma - \Delta$ ADC

In this thesis, we focus on the distributed detection of a binary hypothesis testing problem. For single sensor detection or centralized detection, the sensor node collects N analog noisy observations and preliminarily process the data before communicating with the fusion center. We integrate the complete $\Sigma - \Delta$ ADC model into the sensor node for detection of multiple input observations as the signal processing module. Fig. 2.1 shows the block diagram of a single sensor detection system with $\Sigma - \Delta$ ADC. The noisy observation input into the sensor node at sample time n is,

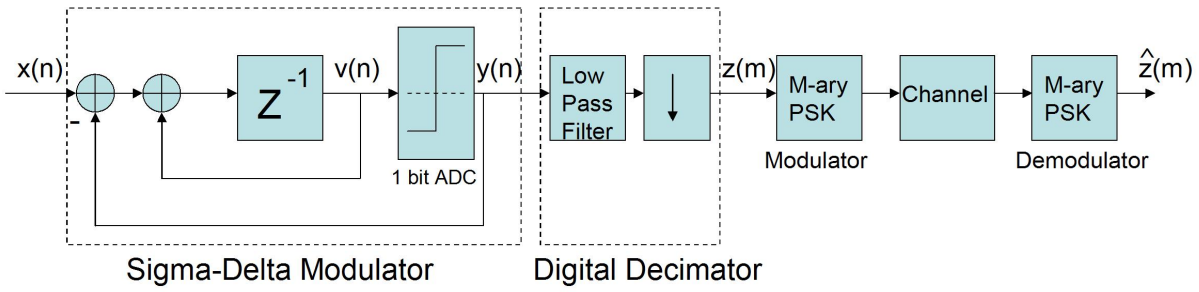

FIGURE 2.1. Single sensor detection with $\Sigma - \Delta$ modulator system model

$$H_1: \quad x(n) = s + w(n), \qquad n = 1, 2, \cdots, N$$
$$H_0: \quad x(n) = w(n), \qquad n = 1, 2, \cdots, N$$

The output of the $\Sigma - \Delta$ modulator $\{y(n)\}_{n=1}^{N}$ is then fed into a digital decimator with decimation factor $K, K < N$, and becomes a multi-bit finite-valued data $z(m)$, $m = 1, 2, \cdots, \lceil K/N \rceil$. M-PSK digital modulation of the bitstream is performed following the digital decimator and the message is then transmitted over an AWGN channel. At the receiver end, signals are demodulated and collected to perform an LR test or other sub-optimal fusion rule like equal gain combining (EGC). The LRT based detection rule and EGC suboptimal fusion rule at the fusion center will be discussed in details in Section 3.2 and Section 4.3. The detection performance depends on the number of input samples N as well as the resolution of the ADC. An alternative system scheme is showed in Fig. 2.2 where the $\Sigma-\Delta$ modulator output $\{y(n)\}_{i=1}^{N}$ are directly modulated and transmitted to the fusion center where final decision will be made based on the received $\{\hat{y}\}_{i=1}^{N}$ directly. As the low-pass filter is removed from the sensor, circuit complexity will be reduced and energy consumed will be saved inside the signal processing module of the sensor. Furthermore, the system detection performance will be improved in the sense that redundant information will be provided to the fusion center through the noisy wireless channel at the cost of transmitting more bits, meaning that more power shall be spent at the communication module.

Simulation results of single sensor detection performance using $\Sigma - \Delta$ ADC are shown in Fig. 2.3. The number of sampled observations is 160 and the transmission power P_t is $20dB$. We chose BPSK modulation at the communication module. The second system model is adopted here so that the number of bits transmitted is also equal to N. We use EGC or average decoder as a global detector throughout this chapter. We use the output

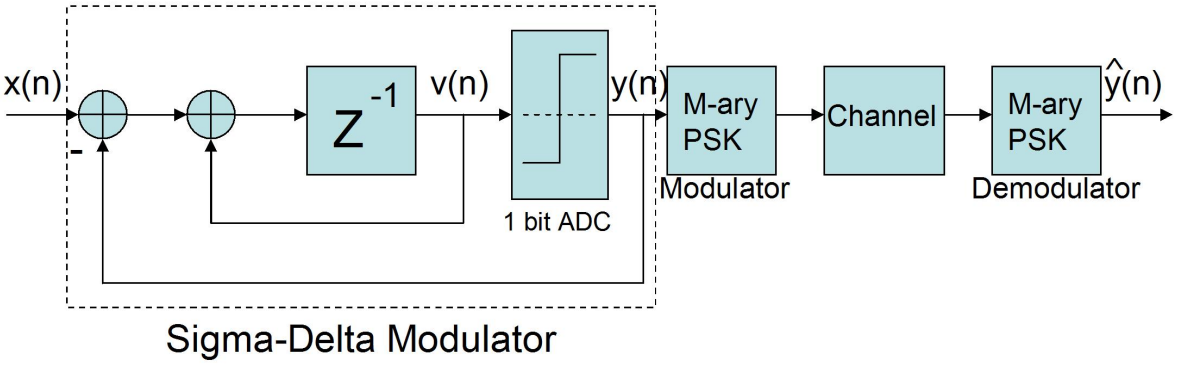

FIGURE 2.2. Single sensor detection with first order $\Sigma - \Delta$ ADC system model, decimator at receiver end

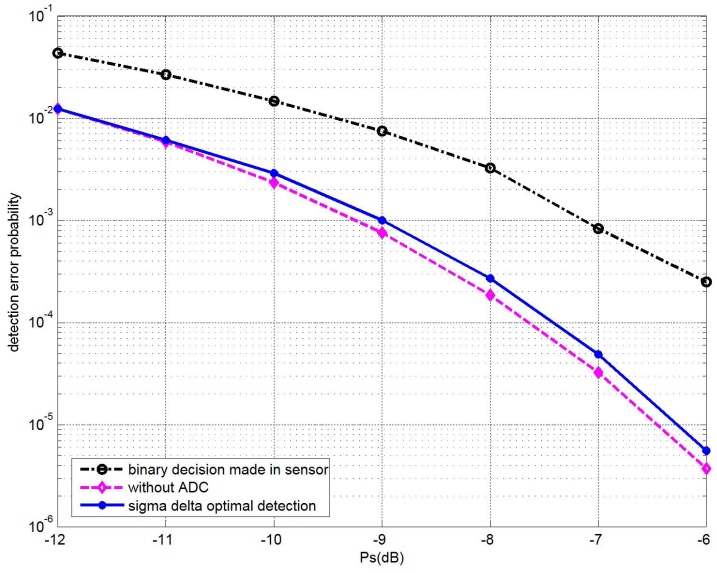

FIGURE 2.3. Single sensor with first order $\Sigma - \Delta$ ADC detection error probability versus P_s, compared to the performance of analog information directly available at fusion center without ADC and channel distortion, P_t=20dB, N=160, BPSK

of the EGC described by

$$Z = \frac{1}{N}\sum_{n=1}^{N}\hat{y}(n)$$

as the detection statistics and make the final decision by the fusion rule

$$\theta = \begin{cases} H_0,\ if\ Z < s/2, \\ H_1,\ if\ Z \geq s/2. \end{cases}$$

The details of the decision fusion rules for distributed detection using $\Sigma-\Delta$ modulation will be discussed in the next two chapters. Detection performance for the case where the analog observations are directly accessible to the fusion center without ADC and channel distortion is provided as benchmark (dash line). Its performance is optimal given the number of samples and the sensor SNR P_s in light of the sufficient statistics argument. Performance of the binary system in which each sensor makes a local binary detection based on each analog observation is also shown for comparison. The detection rule for binary and analog systems will be discussed in Section.3.3. Fig. 2.3 demonstrates that sensor detection with $\Sigma - \Delta$ modulation can outperform the binary system with same number of input samples and binary data transmitted. In addition, it also has performance close to the benchmark of ideal optimal situations.

2.2 Sensor node embedded with a second order $\Sigma - \Delta$ ADC

Another example of single sensor detection using a second order $\Sigma - \Delta$ ADC is discussed in this subsection. Second order $\Sigma - \Delta$ modulation (Fig. 2.4) provides a further shaping of quantization noise spectrum, resulting in a better detection performance. The modulator realize $H_x(z) = z^{-1}$ and $H_e(z) = (1 - z^{-1})^2$. Note that, compared with the first order $\Sigma - \Delta$ noise transfer function, the seconde order noise transfer function provides more quantization noise suppression over the low frequency signal band, and more amplification

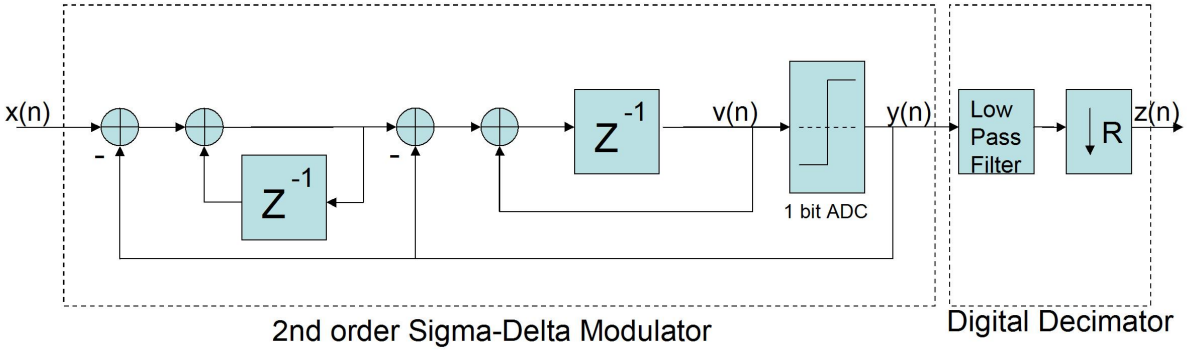

FIGURE 2.4. Second order $\Sigma - \Delta$ modulator AD system

of the noise in the high frequency signal band. The derivation from (1.7) leads to

$$\sigma_{ey}^2 = \int_0^{f_B} P_{ey}(f)df = \int_0^{f_B} \frac{\sigma_e^2}{f_s} H_e(f)df = \sigma_e^2 \frac{\pi^4}{5} (\frac{f_B}{f_s})^5 \tag{2.1}$$

The simulation results shown in Fig. 2.5 give the detection performance of single sensor embedded with second order $\Sigma - \Delta$ ADC versus P_s. With the same parameter set as in the first order $\Sigma - \Delta$ case except that the number of samples taken for one trial of detection is reduced to 48, the single sensor detection system with second order $\Sigma - \Delta$ ADC showed robust performance compared the ideal case that analog signal is directly accessible to the fusion center without ADC. Considering that N is substantially reduced, the conclusion that the second order $\Sigma - \Delta$ ADC will improve the system performance by further eliminating the quantization noise is easily drawn, as expected.

2.3 $\Sigma - \Delta$ modulator with feed forward loop or pre-FIR filter

It has been demonstrated that the essence of the $\Sigma - \Delta$ modulator is to shape the power spectrum of the quantization noise with the feedback loop while keeping the signal power spectrum unaltered before low-pass filtering it so that the 1 bit ADC quantization noise is reduced significantly. For our specific interest of detection, the input signal also contains the sensing noise whose spectrum spreads over the sampling frequency. Our design philosophy

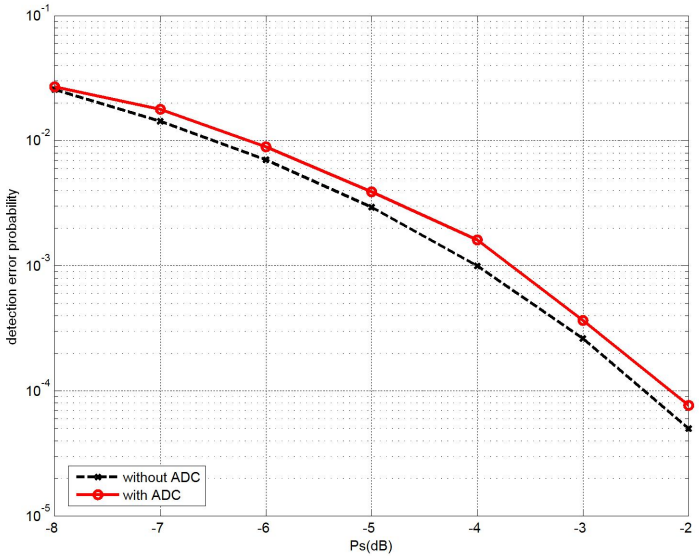

FIGURE 2.5. Detection performance of single sensor with second order $\Sigma - \Delta$ ADC versus P_s, compared to the performance of analog information directly available at fusion center without ADC and channel distortion, P_t=20dB, N=48, 16PSK, Sinc filter, K=16

is to distinguish the two possible inputs rather than recover them, it does no harm to reshape the signal spectrum if we can filter more sensing noise through suitable change in the design. We now introduce one extra feed forward loop in the $\Sigma - \Delta$ modulator in Fig. 2.6.

From the $\Sigma - \Delta$ linear model described in (1.4), the signal transfer function now becomes $a + Z^{-1}$ instead of Z^{-1} which is a low pass filter whereas the noise transfer function remains the same. The total power of the sensing noise is reduced thorough this process. Note that to keep the magnitude response of the low pass filter at one at zero frequency, the output should be scaled down by a factor of $1 + a$.

The simulation result shown in Fig. 2.7 compares the detection performance between the standard $\Sigma - \Delta$ modulator and one with the feed forward loop for different values of a. The number of samples is reduced to 12 in order to show the difference more clearly. There is tremendous improvement on detection performance when the number of samples available

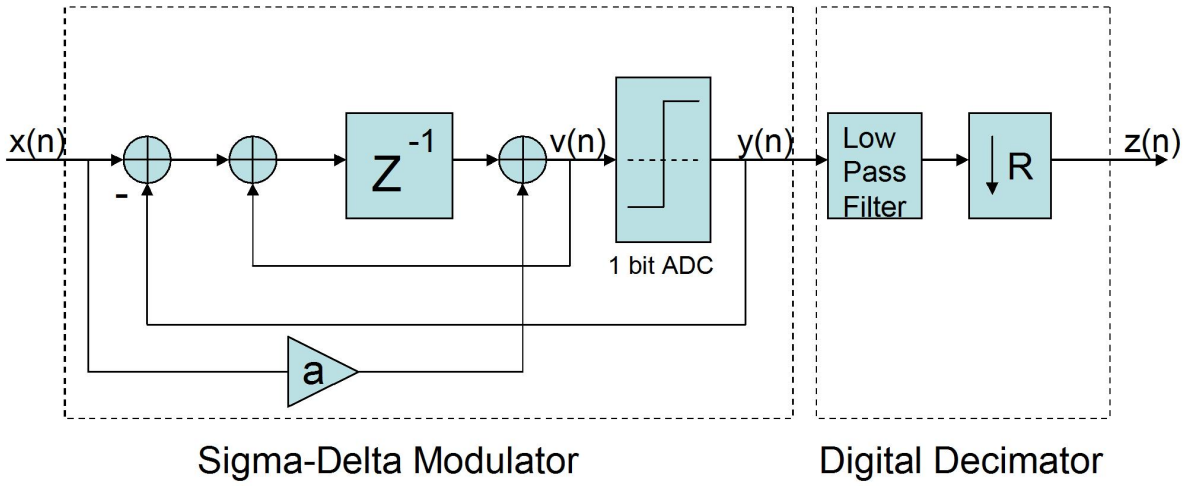

FIGURE 2.6. $\Sigma - \Delta$ modulator with feed forward loop

for one detection is very limited. Performance of the analog system is again provided as a benchmark which assumes analog observations are directly accessible by the fusion center.

We can also adopt this change for the second order $\Sigma - \Delta$ modulator with second order feed forward loop shown in Fig. 2.8. The signal transfer function now becomes

$$H_x(Z) = a + (1 - a + b)Z^{-1} - bZ^{-2}$$

The parameters a and b determine the coefficients of the second order filter $H_x(Z)$ and its frequency response. The simulation results shown in Fig. 2.9 indicate a reduction in probability of error compared to the second order $\Sigma - \Delta$ modulator without feed forward loop as well as the first order $\Sigma - \Delta$ modulator with first order feed forward loop. As expected, the second order $\Sigma - \Delta$ modulation provides further attenuation of the quantization noise power as well as the measurement noise power in the input observation samples. From the simulation we also find the relationship between the detection error probability and the stop frequency θ of the magnitude response of the second order filter $H_x(Z)$, i.e. θ is the angular position of the roots of $|H_x(Z)| = 0$. Since the roots of $a+(1-a+b)Z^{-1}-bZ^{-2} = 0$ are on the unit circle if $ab = -1$ in which case the roots are uniquely specified by angular

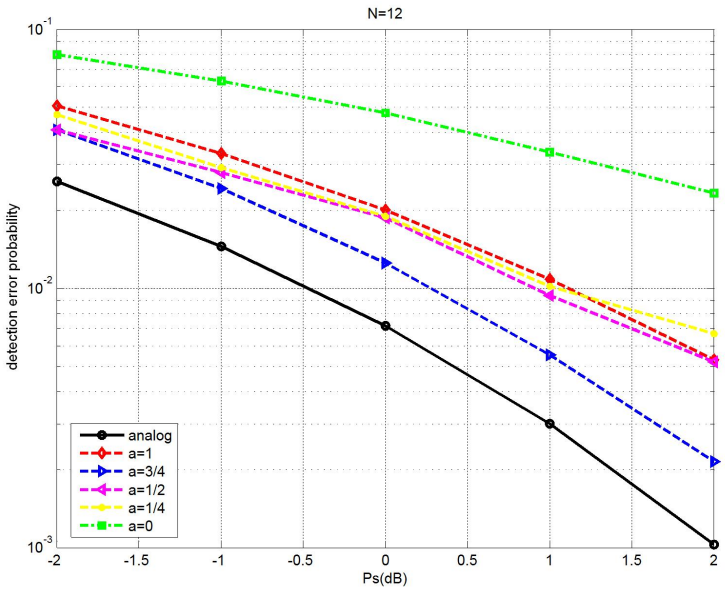

FIGURE 2.7. Single sensor detection performance of $\Sigma - \Delta$ modulator with feed forward loop, N=12, P_t=20dB

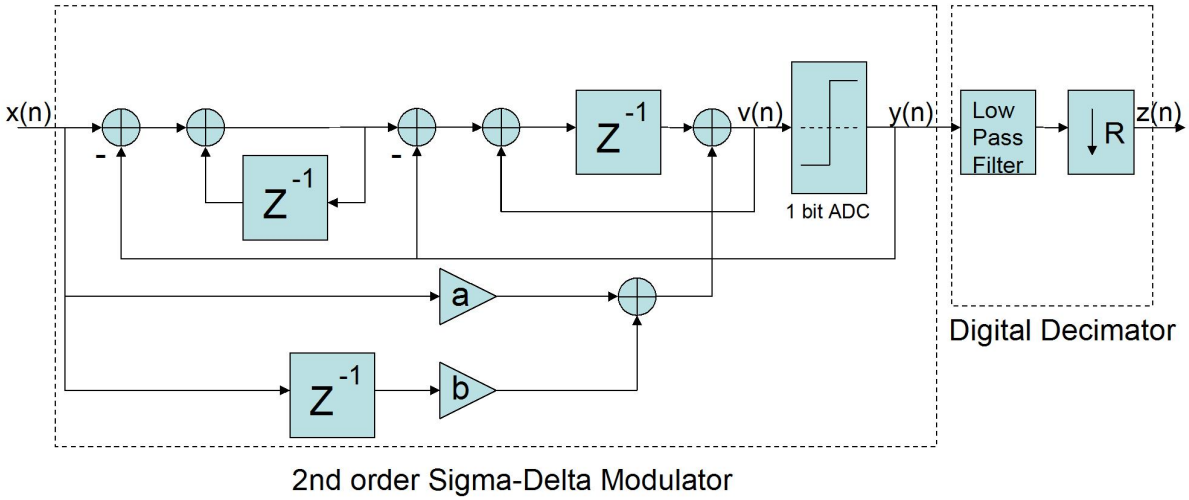

FIGURE 2.8. Second order $\Sigma - \Delta$ modulator with feed forward loop

position θ, we can find the optimal scaling factors in the second order feed-forward link via a sequence of simulations with different values of θ and the corresponding a and b. The results show that the optimal value of a and $b = -a$ in terms of detection performance would be $a = 1$, $b = -1$, $\theta = \frac{2}{3}\pi$ (Fig. 2.10).

In simulations shown in Fig. 2.9, we first compare the detection performance of second order $\Sigma - \Delta$ modulation with feed-forward loop to first order $\Sigma - \Delta$ modulation with feed-forward loop and optimal benchmark. The right figure shows the detection performance of second order $\Sigma - \Delta$ modulation with feed-forward loop of different values of θ, a and $b = -a$. The proper value of a and b will further improve the detection performance.

Since $\Sigma - \Delta$ ADC is a well developed product in industry, it may not be economic to add a loop inside the VLSI chip. Therefore we use another equivalent design to substitute this modification. From (2.1) and Fig. 2.6, the time domain relationship between input and output of the $\Sigma - \Delta$ modulator with a first order feed forward loop can be rewritten as

$$\begin{aligned} v(n+1) &= v(n) - y(n) + x(n) + ax(n-1); \\ y(n) &= q(v(n)); \end{aligned}$$

where

$$q(v) = \begin{cases} 1, & v \geq 0, \\ -1, & v < 0 \end{cases} \tag{2.2}$$

We find this is equivalently a standard $\Sigma - \Delta$ modulator with the input of a colored gaussian sequence $\{\tilde{x}_n | n = 0 \cdots\}$ and $\tilde{x}_n = x_n + ax_{n-1}$. We therefore introduce a pre-FIR filter before the standard $\Sigma - \Delta$ modulator to implement the equivalent feed forward loop, as showed in Fig. 2.11. By intentionally correlating the white input sequence before fed into the standard $\Sigma - \Delta$ modulator, we achieve the same signal modulation as $\Sigma - \Delta$ model with

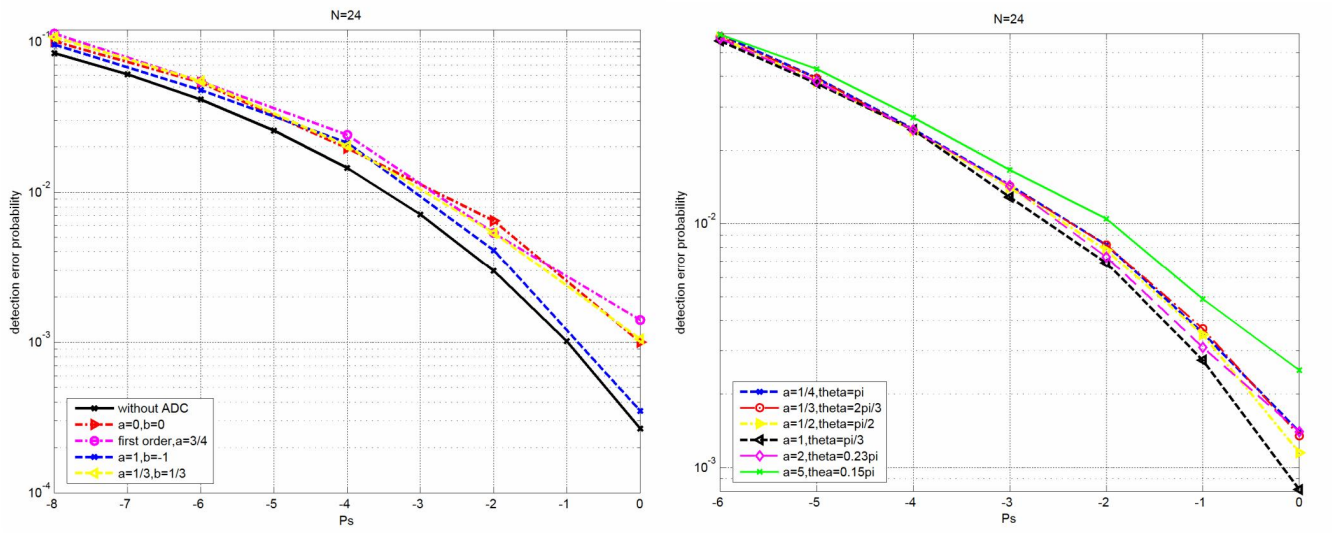

FIGURE 2.9. Single sensor detection performance of second order $\Sigma - \Delta$ modulator with feed forward loop, N=24, P_l=20dB

feed forward loop. Considering the fact that it is easier to implement, this design improves the performance for single sensor detection of i.i.d gaussian input with $\Sigma - \Delta$ ADC.

As motivating examples, our investigation in the single sensor detection shows the potential of employing $\Sigma - \Delta$ modulation in distributed detection. Based on rigorous analysis to be presented in the next two chapters and observations from the simulation results using only a 1-bit quantizer, the $\Sigma - \Delta$ ADC is capable of maintaining and reconstructing the analog observation under the hypotheses to be distinguished. Under distributed detection framework, the time domain approach of the $\Sigma - \Delta$ modulation can be transformed to space domain due to the invariance of the signal. An extra inter-sensor communication link is added to implement the space domain $\Sigma - \Delta$ loop. Moreover, BPSK modulation is a natural choice since each sensor takes only one sample of the observation and transmit only 1 bit information to the fusion center. We will also make use of the soft information at the receiver end instead of hard decision to optimize the detection performance.

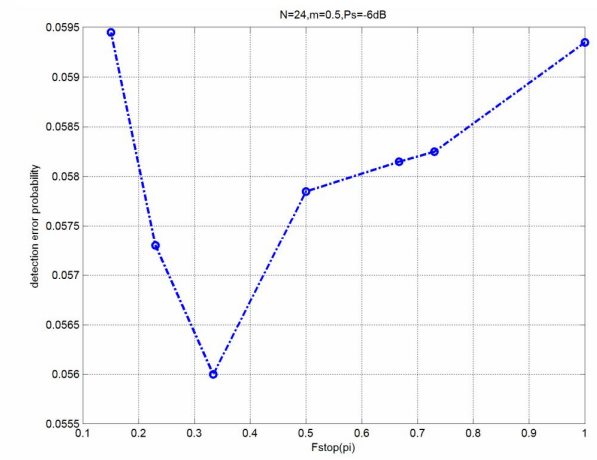

FIGURE 2.10. Detection error probability versus θ when Ps=-6dB, Pt=20dB and N=24

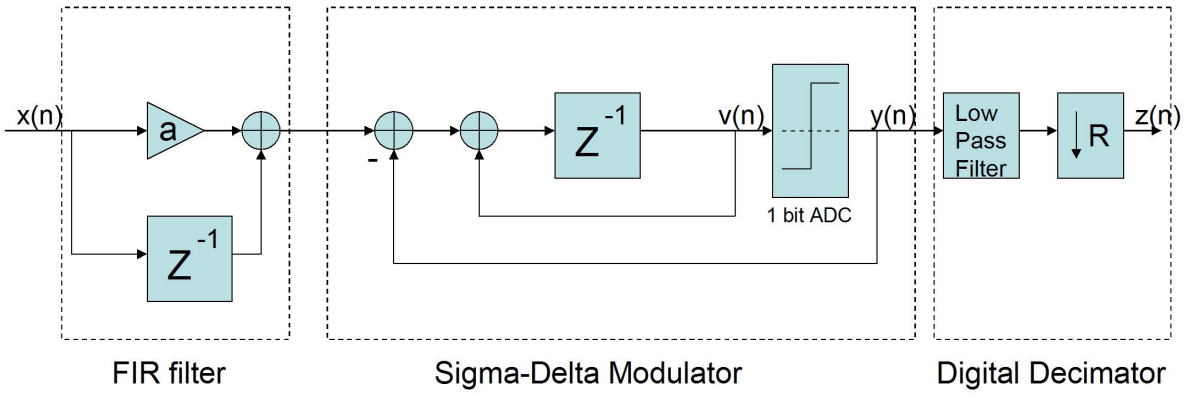

FIGURE 2.11. $\Sigma - \Delta$ Modulator with a pre-FIR filter

Summary

In this chapter, we

- Present the single sensor detection system using the first order and second order $\Sigma - \Delta$ modulation and evaluate the system performances.
- Exploit an additional feed forward loop or a pre-FIR filter block in $\Sigma - \Delta$ modulator block to improve the system performance.

Chapter 3

$\Sigma - \Delta$ modulation based distributed detection in AWGN channels

3.1 System model

Suppose that there are N sensor nodes observing a random phenomenon. Each sensor collects only one noisy observation described by

$$\begin{aligned} H_1: \quad & x_i = s + w_i, \qquad i = 1, 2, \cdots, N \\ H_0: \quad & x_i = w_i, \qquad\quad i = 1, 2, \cdots, N \end{aligned}$$

where s is a known constant signal and $\{w_1, w_2, \cdots, w_N\}$ are measurement noises that are mutually independent and identically distributed as real Gaussian random variables with mean zero and variance σ_w^2. Different from distributed detection systems with parallel topology, we also allow communication between adjacent sensor nodes. As a result, the N-sensor actually follows a mixing of serial and parallel topology as shown in Fig. 3.1. For this topology, sensor node i maps its local observation x_i and the signal v_{i-1} sent by the adjacent sensor node $i-1$ to its output $(v_i, y_{i-1}) = \gamma_i(x_i, v_{i-1})$, in which y_{i-1} is then transmitted to a fusion center respectively over a unique assigned channel (e.g. a time slot). v_i which carries the information of the ith observation is then transmitted to the next sensor node over another assigned orthogonal channel. The received signal at the fusion center from the ith sensor node is given by

$$\hat{y}_i = y_i + n_i, \quad i = 1, \cdots, N \tag{3.1}$$

where n_i is AWGN with variance σ_n^2.

The fusion center receives $\{\hat{y}_1, \hat{y}_2, \cdots, \hat{y}_N\}$ and makes a global decision θ based on an optimal or suboptimal fusion rule which will be discussed in the next two sections. The detection performance is characterized by the detection error probability in (1.1) with respect to the sensor measurement SNR $P_s \triangleq s^2/\sigma_w^2$ denoted and the inter-sensor channel

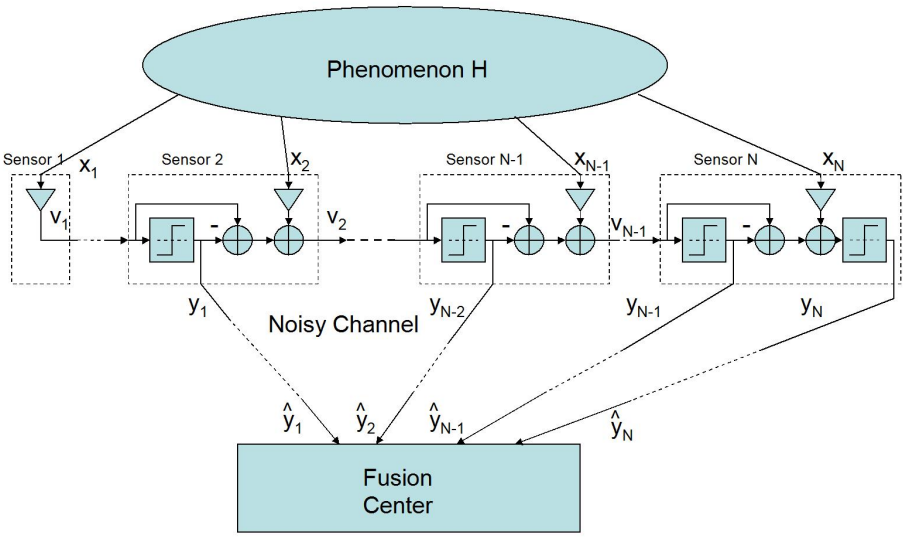

FIGURE 3.1. $\Sigma - \Delta$ modulation based distributed detection system model

SNR (with normalized transmission power $1/\sigma_n^2$) denoted by $P_t = 1/\sigma_n^2$. With the statistic knowledge of w_i, h_i, n_i, the optimal fusion rule at the fusion center is the LRT rule described in (1.2).

We now consider to integrate the $\Sigma - \Delta$ modulator into the sensor node as a local quantizer with only 1 bit resolution. From the motivation example of single sensor detection system using $\Sigma - \Delta$ ADC presented in Chapter 2, in which we provided details of how to integrate the $\Sigma - \Delta$ ADC as a signal modulation and processing module into sensor design, we extend the application to distributed detection, we need the extra communication link between sensor nodes to implement the space domain $\Sigma - \Delta$ loop.

The fusion center uses the output bit stream of the modulator that represents the analog observation to make a binary decision. From Fig. 1.2 the relationship between the input and output of the $\Sigma - \Delta$ modulator is given by

$$\begin{aligned} v_{i+1} &= x_i - y_i + v_i, \\ y_i &= q(v_i). \end{aligned} \tag{3.2}$$

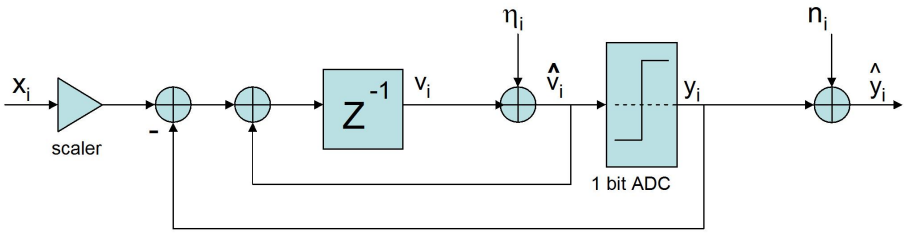

FIGURE 3.2. Equivalent model for $\Sigma - \Delta$ modulation based distributed detection system over AWGN channels

where

$$q(v) = \begin{cases} 1, & v \geq 0, \\ -1, & v < 0 \end{cases} \tag{3.3}$$

assuming that the output of the one bit quantizer is either 1 or -1. For the detection purpose, we drop the oversampling block in the $\Sigma - \Delta$ modulator due to the following reason: Our purpose is not to reconstruct the analog input signal x_i, but to distinguish between two hypothesis; Without oversampling, the spectrum of the measurement noise in x_i is spread in the same way as the quantization noise spectrum, most of which will be filtered by the subsequent decimator. We also add a scaler block in front of the modulator to optimize the detection performance which will be discussed in detail in Section 3.3.

Fig. 3.1 shows the $\Sigma - \Delta$ modulation based distributed detection scheme and Fig. 3.2 shows its equivalent model. Assume that each sensor node takes only one sample of x_i. Since the time domain approach of the $\Sigma - \Delta$ modulation can be transformed to spacial domain, we implement the $\Sigma - \Delta$ modulation in the distributed sensor network with a combination of serial and parallel topology [2]. The ith sensor node transmits y_{i-1} to the fusion center and v_i to the $(i+1)$th sensor node over an inter-sensor AWGN channel with power P_I and

$$P_I = \frac{E(v_i^2)}{\sigma_\eta^2} \tag{3.4}$$

where $E(v_i^2)$ will be given in Section 3.2 and σ_η^2 is the variance of AWGN η_i. We assume no fading in the inter-sensor channels throughout the thesis because of the close distance between adjacent sensor nodes. At the $(i+1)$th sensor node, $v_i + \eta_i$ is quantized to obtain y_i. The $(i+1)$th sensor uses $v_i + \eta_i$ and y_i as the feedback to generate v_{i+1}, meanwhile transmitting y_i to the fusion center and v_{i+1} to the next sensor node. Therefore we form an equivalent $\Sigma - \Delta$ modulator loop within the sensor network. The fusion center will use $\{\hat{y}_1, \hat{y}_2, \cdots, \hat{y}_N\}$ to perform detection. By modifying (3.2), this process can be characterized by,

$$\begin{aligned} v_{i+1} &= x_i - y_i + v_i + \eta_i, \\ y_i &= q(v_i + \eta_i). \end{aligned}$$

Note that the 1st sensor does not output and the last sensor produces two outputs y_{i-1} and y_i to the fusion center.

3.2 Fusion rule for $\Sigma - \Delta$ modulation based distributed detection system

We first investigate our proposed scheme and develop a suboptimal detection algorithm. A closed-form solution to the detection error probability is obtained for the algorithm.

WLOG, we assume $\pi_0 = \pi_1$. The optimal fusion rule is the likelihood ratio test (LRT) based fusion rule [28]. It requires the joint pdf of y_i and $\hat{y}_i$ in order to compute the likelihood ratio in (1.2). We will develop the LRT based fusion algorithm in Section 4.3. However, the LRT does not yield any insight regarding the performance discrepancy between different approaches. Therefore we will adopt a suboptimal fusion rule first and for AWGN channel it has close performance to the LRT fusion rule.

In [23], it was shown that averaging $\{y_i\}_{i=1}^N$ is an efficient decoder that functions as a digital decimator for single loop $\Sigma - \Delta$ modulators with i.i.d Gaussian input. This result inspires us to employ a simple form of equal gain combiner (EGC) $Z := \frac{1}{N}\sum_{i=1}^N \hat{y}_i$ as

our detection statistics. The averaging of $\{\hat{y}_i\}_{i=1}^N$ is compared with a threshold which will be shown to be $s/2$ later. Although the results in [23] are obtained for traditional $\Sigma - \Delta$ ADC with i.i.d Gaussian inputs, our simulation results demonstrate that it is a good approximation when inter-sensor SNR is reasonably high.

3.2.1 Statistics of binary quantizer error in $\Sigma - \Delta$ modulation with i.i.d Gaussian input

Applying the analog observation signal model in (3.1) and assuming it has already been scaled before fed into the $\Sigma - \Delta$ loop inside each sensor node, without the inter-sensor noise, we rewrite (3.2) and obtain

$$v_{i+1} = v_i - q(v_i) + m + w_i \tag{3.5}$$

where $m = 0$ under H_0 and $m = s$ under H_1. The desired LR $\frac{f(Z|H_0)}{f(Z|H_1)} = \frac{f(Z|m=0)}{f(Z|m=s)}$. Denote $\lambda(v) := v - q(v) + m$. We can transform the quantization error by defining $\bar{e}_i := \lambda(v_i)$. Now (3.5) can be written as $v_i = \bar{e}_{i-1} + w_{i-1}$ that yields the recursion:

$$\bar{e}_{i+1} = \lambda(\bar{e}_i + w_i)$$

It is proved in [23] that the process $\bar{\mathbf{e}} = \{\bar{e}_i | i = 0, 1, ...\}$ is a real valued discrete-time Markov process and it has a unique invariant probability measure if and only if $|m| < 1$. Note for $|m| \geq 1$, we can always scale accordingly the quantization level in (3.3) to make the equivalent $m < 1$. For $n \geq 1$ $\bar{e}_i$ can be represented as

$$\bar{e}_i = \bar{e}_{i-1} - erf(\bar{e}_{i-1}/\sqrt{2}\sigma_w) + m + \xi_i \tag{3.6}$$

where $\{\xi_i\}_{i\geq 1}$ is an uncorrelated sequence of random variables (innovations) with zeros means and

$$erf(x/\sqrt{2\sigma_w^2}) = 2\int_{-\infty}^{x} (1/\sqrt{2\pi}\sigma_w) e^{-t^2/2\sigma_w^2} dt - 1$$

Moreover, $\bar{e}_i$ can be split into two independent random variables

$$\bar{e}_i = g_i + m + o_i$$

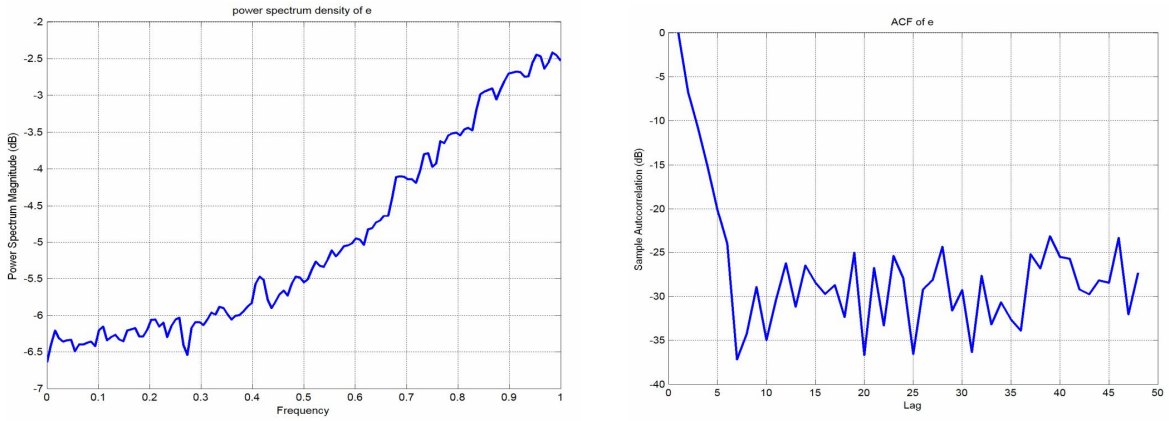

FIGURE 3.3. An example of $\Sigma - \Delta$ binary quantizer error power spectrum and autocorrelation function under granular mode

The random variable g_i is referred as"granular noise" which is uniformly distributed over the interval $[-1, 1]$, and o_i as "slope overload noise". In the time domain, o_i is the reconstruction error due to that the single-loop modulator can only estimate the input by steps of magnitude 1 while g_i is simply due to the coarseness of the 1 bit quantizer and that $q(v_i)$ changes its sign often. In the frequency domain, o_i is concentrated in the high-frequency end of the spectrum while g_i is concentrated in the low-frequency end, which are referred as granular mode and slope overload mode respectively.

The spectral density $s_{\bar{e}}(\Omega)$ is given by [23]

$$s_{\bar{e}}(\Omega) = \frac{1}{2\pi}|\beta(\Omega)|^2 v(\Omega) \tag{3.7}$$

where the Markovian model corresponds to $v(\Omega) = 1$ and

$$\beta(\Omega) = \frac{1-\gamma^2}{1+\gamma^2-\gamma\cdot\cos(\Omega)} \tag{3.8}$$

The parameter γ is the linear recursion factor in the first-order Markov model $\bar{e}_i = \gamma \cdot \bar{e}_{i-1} + \xi_i/\sigma_w$ which can be approximated as

$$\gamma = (1 - 2b/\sqrt{\pi} + b/2\sqrt{\pi} \cdot (4\sigma_w^2 - 2)) \tag{3.9}$$

and is restricted by the condition

$$-1 < \gamma < 1 \tag{3.10}$$

where b is the quantization level and in this thesis b is normalized to 1. From the (3.7)-(3.9) we can see the influence of granular and slope overload noise on the spectrum of $\bar{e}_n$, elaborated as follows. Large values of the quantizer step b makes γ satisfying (3.10) negative and the spectral density in (3.8) as well as (3.7) is concentrated in the high-frequency end of $[0, \pi/2]$, when the granular noise is dominant, while small values of b makes γ positive and the spectral density is concentrated in the low-frequency end of $[0, \pi/2]$. Since the quantization step is fixed to 1, large $|m|$ and σ_w^2 makes quantization step small in the sense that there are a large number of input samples that exceed b and the modulator predicts the input with a relatively small b and renders the error spectral in the slope overload mode. An example of $\Sigma - \Delta$ binary quantizer error power spectrum and autocorrelation function under granular mode is shown in Fig. 3.3.

3.2.2 Detection error probability using Equal gain combiner as the suboptimal detector

We now assume that the $\Sigma - \Delta$ modulation in distributed detection is under granular mode, meaning the auto correlation function of $\bar{e}_i$ will fall to zero rapidly with large N. This is reasonable since v_i will not be large enough to produce the slope overload noise. This assumption is extended to our distributed detection scheme even though now inter-sensor noise η_i is included in the $\Sigma - \Delta$ recursion.

For the distributed detection scheme in Fig. 3.1 and Fig. 3.2, after including inter-sensor channels, we can modify (3.5) as

$$v_{i+1} = v_i + \eta_i - q(v_i + \eta_i) + m + w_i \tag{3.11}$$

where η_i is the white Gaussian noise in the inter-sensor channel with variance $\sigma_\eta^2 = E(v_i^2)/P_t$.

The binary quantizer error $\bar{e}_i$ is modified as

$$\bar{e}_i = v_i + \eta_i - q(v_i + \eta_i) + m. \tag{3.12}$$

We still approximate $\bar{e}_i$ as

$$\bar{e}_i \approx g_i + m$$

with stationary uniform distribution between $[m+1, m-1]$. Then we can write the power of v_i as

$$E(v_i^2) = E(\bar{e}_i^2) + \sigma_w^2 = 1/3 + s^2/2 + \sigma_w^2$$

Combining (3.11), (3.12) and (3.1) yields

$$y_{i+1} = q(v_{i+1} + \eta_{i+1}) = m + w_i + \eta_{i+1} + \bar{e}_i - \bar{e}_{i+1} \tag{3.13}$$

$$\hat{y}_{i+1} = y_{i+1} + n_{i+1} = m + w_i + n_i + \eta_{i+1} + \bar{e}_i - \bar{e}_{i+1} \tag{3.14}$$

At the fusion center, upon receiving $\{\hat{y}_1, \cdots, \hat{y}_N\}$, we use Equal Gain Combiner (EGC) as the suboptimal detector and its output to perform the LRT detection. To write the output Z of EGC explicitly,

$$Z = \frac{1}{N}\sum_{i=1}^{N}(\hat{y}_i) = \frac{1}{N}\sum_{i=1}^{N}(y_i + n_i) \tag{3.15}$$

where n_i is the noise of channel from sensor node to the fusion center with variance $\sigma_n^2 = 1/P_t$.

From (3.14) we can see why EGC is an efficient decoder for $\Sigma - \Delta$ modulator since it cancels most of the quantization error part in the output bit stream. In frequency domain, it performs a low-pass filtering to the quantization noise whose power is concentrated in the high frequency end under granular mode assumption. Combing (3.15) and (3.14), we obtain the detection statistics,

$$\bar{n} = \frac{1}{N}[\sum_{i=0}^{N-1}(w_i + \eta_i + n_i)] + \frac{1}{N}(\bar{e}_0 - \bar{e}_N), \tag{3.16}$$

where $\bar{n} := Z - m$. The first term in (3.16) is a zero-mean Gaussian random variable with variance $\sigma^2 = \frac{1}{N}(\sigma_w^2 + \sigma_\eta^2 + \sigma_n^2)$ where $\sigma_w^2 + \sigma_\eta^2 + \sigma_n^2$ is referred as the total noise power. Under granular mode $\bar{e}_0 - \bar{e}_N$ can be replaced by $g_0 - g_N$. Denote

$$\hat{e} := \frac{1}{N}(\bar{e}_0 - \bar{e}_N) \tag{3.17}$$

as the detection-wise quantization error. When N is large enough such that the correlation between g_0 and g_N is very weak, $\hat{e}$ becomes the sum of two i.i.d random variables uniformly distributed over $[-1/N, 1/N]$ with power $E(\hat{e}^2) = \frac{2}{N^2}E(g_i^2) = \frac{2}{3N^2}$. Its pdf is a triangular waveform given by

$$f_{\hat{e}}(x) = \begin{cases} \frac{1}{4}N^2x + \frac{N}{2}, & x \in [-2/N, 0], \\ -\frac{1}{4}N^2x + \frac{N}{2}, & x \in [0, 2/N]. \end{cases}$$

Since the noise w_i, η_i, n_i are mutually independent and are all independent of $\bar{e}_i$. The pdf of $\bar{n}$ for large N can thus be approximated as the convolution of a zero-mean Gaussian pdf with variance σ^2, denoted as $\Psi(x)$ and the triangular waveform function $f_E(x)$,

$$\begin{aligned} f_{\bar{n}}(y) &= \int_{-\infty}^{\infty} \Psi(x) f_{\hat{e}}(y - x)dx \\ &= \frac{N^2\sigma}{4\sqrt{2\pi}}[e^{\frac{-(y-\frac{2}{N})^2}{2\sigma^2}} + e^{\frac{-(y+\frac{2}{N})^2}{2\sigma^2}} - 2e^{\frac{-y^2}{2\sigma^2}}] + \frac{N^2}{4}[2yQ(\frac{y}{\sigma}) \\ &\quad -(y - \frac{2}{N})Q(\frac{(y - 2/N)}{\sigma}) - \frac{N^2}{4}(y + \frac{2}{N})Q(\frac{(y + 2/N)}{\sigma})] \end{aligned} \tag{3.18}$$

where $Q(x) = \frac{1}{\sqrt{2\pi}}\int_x^\infty e^{-\frac{t^2}{2}}dt$.

It can be seen that $f_{\bar{n}}(y)$ is an even function. Consequently, the pdf of Z under each hypothesis is $f_{\bar{n}}(Z - m)$, which is concentrated over 0 or s. The standard LRT rule gives us the detection threshold $y_0 = s/2$ and the decision rule based on EGC output Z,

$$\theta = \begin{cases} H_0, \ if \ Z < s/2, \\ H_1, \ if \ Z \geq s/2. \end{cases}$$

Then the detection error probability is derived as,

$$
\begin{aligned}
P_{e,N,\Sigma-\Delta} &= \int_{y_0}^{\infty} f_{\bar{n}}(y)dy \\
&= \int_{y_0}^{\infty}\int_{y-\frac{2}{N}}^{y} \Psi(x)[\frac{1}{4}N^2(x-y)+\frac{N}{2}]dxdy + \int_{y_0}^{\infty}\int_{y}^{y+\frac{2}{N}} \Psi(x)[-\frac{1}{4}N^2(x-y)+\frac{N}{2}]dxdy \\
&= \int_{y_0-\frac{2}{N}}^{y_0} \Psi(x)\int_{y_0}^{x+\frac{2}{N}} [\frac{1}{4}N^2(x-y)+\frac{N}{2}]dydx + \int_{y_0}^{\infty}\Psi(x)\int_{x}^{x+\frac{2}{N}} [\frac{1}{4}N^2(x-y)+\frac{N}{2}]dydx
\end{aligned}
$$

The result of the integral yields

$$P_{e,N,\Sigma-\Delta} = \frac{N^2}{8}A + \frac{N^2\sigma}{8\sqrt{2\pi}}B \tag{3.19}$$

where

$$A = [(y_0-\tfrac{2}{N})^2+\sigma^2]Q(\tfrac{(y_0-2/N)}{\sigma}) + [(y_0+\tfrac{2}{N})^2+\sigma^2]Q(\tfrac{(y_0+2/N)}{\sigma}) - 2(y_0^2+\sigma^2)Q(\tfrac{y_0}{\sigma})$$

and

$$B = 2y_0 e^{\frac{-y_0^2}{2\sigma^2}} - (y_0-\tfrac{2}{N})e^{\frac{-(y_0-\frac{2}{N})^2}{2\sigma^2}} - (y_0+\tfrac{2}{N})e^{\frac{-(y_0+\frac{2}{N})^2}{2\sigma^2}}$$

This closed form solution gives a good approximation to the system detection error probability if N is large, as shown by the simulation results in Fig. 3.4. From (3.16),(3.18) and (3.19) we can also get some insights regarding the detection performance with respect to various parameters P_s, P_t, P_I, s and N. The three independent white Gaussian noise w_i, n_i and, η_i make the same contribution to the detection performance and it does not yield the same performance with fixed P_s while $y_0 = s/2$ varies. The other noise we are dealing with is the detection-wise quantization error $\hat{e}$ in (3.17)and its power falls to zero at a rate of N^2 while the gaussian noise part fall to zero at a rate of N. Applying the central limit

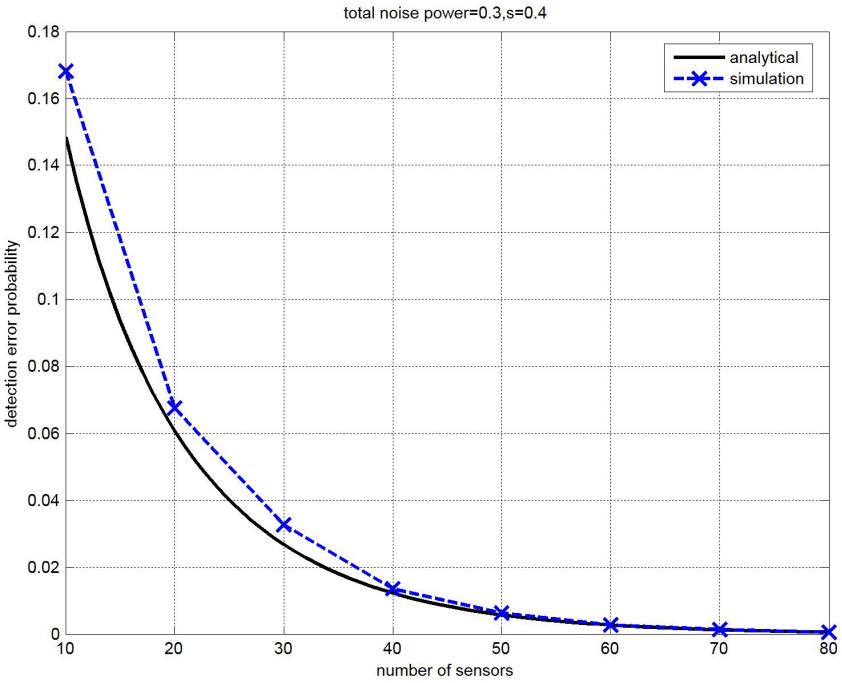

FIGURE 3.4. Analytical and simulation results for detection error probability in (3.19) versus N of the $\Sigma - \Delta$ modulation based distributed detection system in AWGN channels, P_t=10dB, P_I=15dB, P_s=-2dB, s=0.4

theorem (CLT), the detection-wise signal to noise ratio of Z can be simplified to a form under Gaussian approximation,

$$SNR = \frac{s^2}{\frac{(\sigma_w^2+\sigma_n^2+\sigma_\eta^2)}{N} + \frac{2}{3N^2}} \tag{3.20}$$

Replace σ_w^2 with $\frac{s^2}{P_s}$ in the above formula. It is clear that with fixed other parameters, the signal to noise ratio as well as the detection performance is monotonicly increasing with s until it exceeds 1 or the modulator is under slope overload mode. Therefore, it is very important to place a scaler block in front of the modulator in each sensor to ensure s is scaled to a proper value in the sense that we can achieve an optimum performance if the quantization level is set to 1.

3.3 Fusion rule for Binary and Analog distributed detection system

We consider comparing the detection performance of our proposed scheme under the mixing topology with that of binary and analog approaches under the parallel topology for sensor nodes.

Binary system

In binary distributed detection systems under parallel topology, each sensor node locally makes a binary decision by comparing the measurement x_i with the threshold of $s/2$ and then transmits the binary message to the fusion center. The LR of $\{\hat{y}_i\}_{i=1}^N$ at the fusion center under two hypothesis can be easily derived as,

$$\begin{aligned}
\Lambda &= \prod_{i=1}^{N} \frac{f(\hat{y}_i|H_0)}{f(\hat{y}_i|H_1)} \\
&= \prod_{i=1}^{N} \frac{f(\hat{y}_i|y_i=1)P(y_i=1|H_0) + f(\hat{y}_i|y_i=-1)P(y_i=-1|H_0)}{f(\hat{y}_i|y_i=-1)P(y_i=-1|H_1) + f(\hat{y}_i|y_i=1)P(y_i=1|H_1)} \\
&= \prod_{i=1}^{N} \frac{P_f e^{-\frac{(\hat{y}_i-1)^2}{2\sigma_n^2}} + (1-P_f)e^{-\frac{(\hat{y}_i+1)^2}{2\sigma_n^2}}}{P_f e^{-\frac{(\hat{y}_i+1)}{2\sigma_n^2}} + (1-P_f)e^{-\frac{(\hat{y}_i-1)}{2\sigma_n^2}}}
\end{aligned} \tag{3.21}$$

where $P_f = Q(s/2\sigma_w)$ is the local detection error probability. Note that false alarm probability and false detection probability are equal in this case. The optimal LRT fusion rule is thus straightforward to implement using (1.2). Simulation results for binary system detection performance will be provided in Section 3.4.

In order to further analyze the binary detection system performance, we also investigate in a suboptimal fusion rule that use the demodulated hard information at the fusion center for detection. The LR of the received hard information can be written as

$$\Lambda = \prod_{i=1}^{N} W_i$$

where

$$W_i = \begin{cases} \phi = (\frac{(1-P_f)(1-P_b)+P_fP_b}{(1-P_f)P_b+P_f(1-P_b)}, & \text{if} \quad \hat{y}_i = 1 \\ \frac{1}{\phi}, & \text{if} \quad \hat{y}_i = -1 \end{cases}$$

where $P_b = Q(\frac{1}{\sigma_n})$ is the communication bit error probability of BPSK modulation system. Denote $N_{\{\hat{y}_i\}_{i=1}^N=-1}$ the number of -1s in the demodulated $\{\hat{y}_i\}_{i=1}^N$. It is easy to show that $\Lambda > 1$ when $N_{\{\hat{y}_i\}_{i=1}^N=-1} > N/2$. The LRT detection rule based on the hard information $\{\hat{y}_i\}_{i=1}^N$ can thus be obtained by a majority vote,

$$\gamma_0(\hat{y}_1, \cdots, \hat{y}_N) = \begin{cases} H_0, & \text{if} \quad N_{\{\hat{y}_i\}_{i=1}^N=-1} \geq N/2 \\ H_1, & else \end{cases}$$

The detection probability error probability at fusion center thus can be written explicitly as

$$P_{e,N,B} = \sum_{i=\lceil \frac{N}{2} \rceil}^{N} (\tbinom{N}{i}) P_{te}^i (1 - P_{te})^{(N-i)} \tag{3.22}$$

where $P_{te} = P_f + P_d - P_fP_d = Q(\frac{s}{2\sigma_w}) + Q(\frac{1}{\sigma_n}) - Q(\frac{s}{2\sigma_w})Q(\frac{1}{\sigma_n})$ is the detection error probability from single sensor node and $\lceil x \rceil$ is the smallest integer greater than x.

Binary system has been extensively studied in recent years. Channel aware distributed detection was brought up in [9, 10, 11] that integrate wireless channel conditions in local sensor design. Under the framework of this thesis, the channel aware design means the local mapping rules $\{\gamma_1, \gamma_2, \cdots, \gamma_N\}$ should be jointly selected with the global optimal fusion rule at the fusion center, adaptive to the channel conditions $f(\hat{y}_1, \cdots, \hat{y}_N | y_1, \cdots, y_N, H_j)$. For local binary decision, optimal LRT decision rule does not necessarily yields global optimal detection performance. However, since both local observations and channel conditions are i.i.d, we will only consider i.i.d local optimal decision rule for such homogeneous networks, with global LRT decision rule at the fusion center, and we will use it to compare with our proposed system.

Analog System

The second type of transmission mapping strategy at local sensor is that each sensor node retransmits a scaled version of its own analog observation. The receive signal at the fusion center from sensor i can be written as,

$$\hat{y}_i = \alpha(m + w_i) + n_i$$

where α is the scaling factor that ensures its unity transmission power and $\alpha = \sqrt{\frac{2}{s^2+2\sigma_w^2}}$. Since it is an independent Gaussian random variable with mean αm and variance $(\alpha\sigma_w)^2 + \sigma_n^2$, detection error probability for N sensors can be written explicitly as,

$$P_{e,N,A} = Q\left(\frac{\alpha s/2}{\sqrt{(\alpha^2\sigma_w^2 + \sigma_n^2)/N}}\right) \tag{3.23}$$

Fig. 3.5 illustrates that under which circumstance the two strategy would have lower probability of error. For analytical purpose we compare optimal analog detection performance with suboptimal binary detection performance using hard decision. However the conclusion will still hold for binary soft decision WLOG. As the number of sensors grows, the detection performance for analog communication dominant over transmitting binary decisions when P_t is large and P_s is small. This can be intuitively explained in the sense that on one hand, when the communication link is very good, i.e. the fusion center have all the data from every sensor almost error free, r_i^N would be the sufficient statistics for the detection of H_1 and H_2, on the other hand when the noise at each sensor for local decision is overwhelming, the local detection error is too large making the binary local decision, suggesting it is better to collect all the analog data together at fusion center for one detection with less probability of error. This evaluation matches the results presented in [8] which provide the asymptotic detection performance comparison between analog and binary system using large deviation technique.

Comparison of the three schemes will be discussed in Section 3.4.

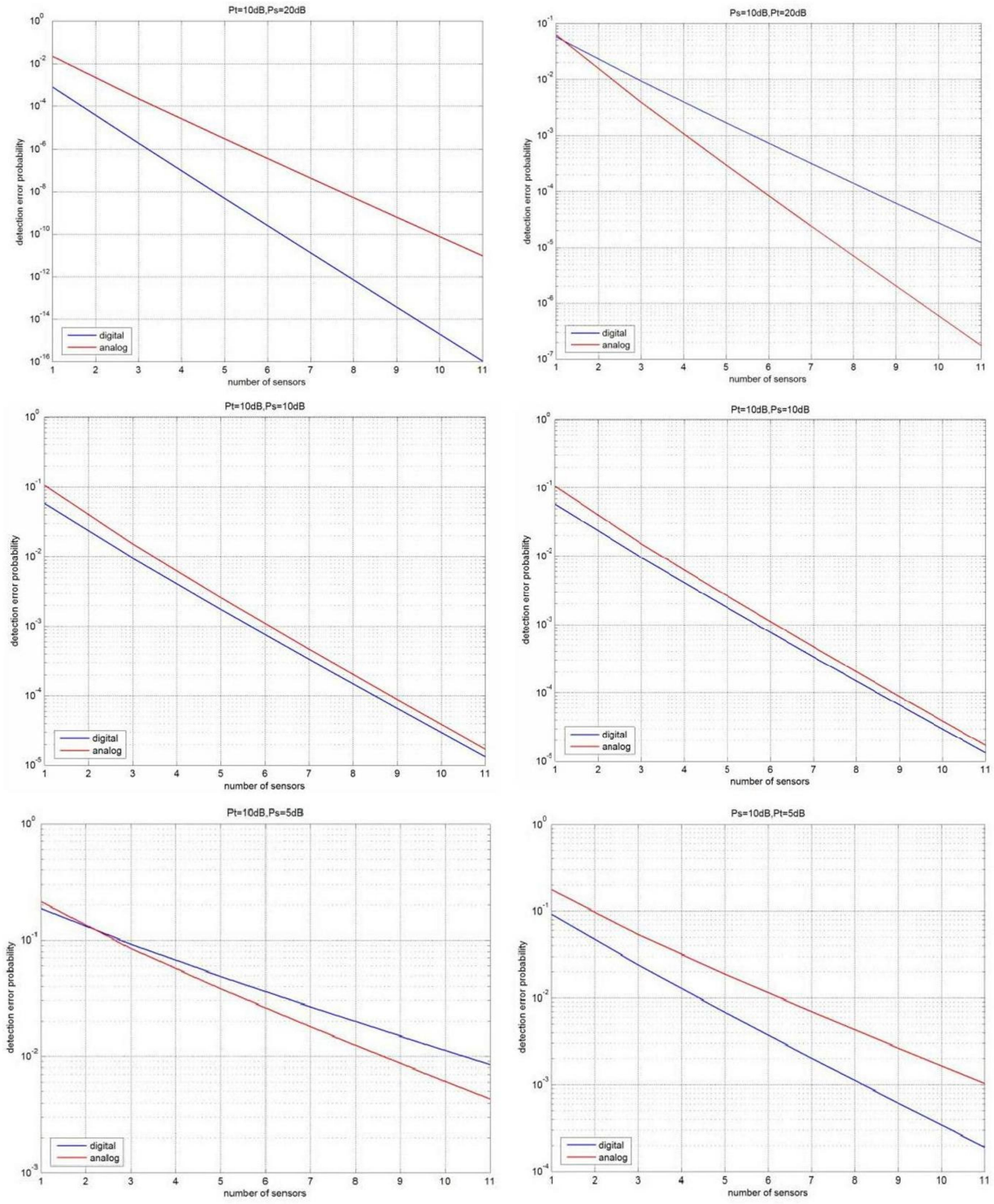

FIGURE 3.5. Analytical detection performance comparison between analog and binary system using (3.22) and (3.23)

3.4 Performance evaluation

In this section we compare the performance of our proposed $\Sigma - \Delta$ modulation based distributed detection system with that of binary and analog system in terms of detection error probabilities.

Fig. 3.6, Fig. 3.7 and Fig. 3.8 illustrate the detection performance of three distributed detection systems as a function of P_s, P_t, N in AWGN channels, respectively. In Fig. 3.6, simulation results are provided for binary system using the optimal soft decision described in (3.21) while numerical results are provided for analog and $\Sigma-\Delta$ modulation based system using (3.23) and (3.19). In this way, we can compare fairly the performance of the three performance with the optimal soft decision fusion rule. In Fig. 3.7 and Fig. 3.8, we use (3.22) for binary system with optimal hard decision to present numerical comparison of the three systems. From these figures we can see that $\Sigma - \Delta$ modulation based distributed detection system can outperform both the analog and the binary distributed detection system under certain conditions. To better understand this, let us neglect $\bar{e}_0 - \bar{e}_N$ and inter-sensor channel noise η_i in (3.16). This is reasonable when σ_n^2, σ_w^2 and N are large. In addition, inter-sensor channel link is assumed to be good due to the close distance between adjacent sensor nodes. Hence the detection symbol Z can be approximated as $m + \frac{1}{N}[\sum_{i=0}^{N-1}(w_i + n_i)]$. This is exactly the detection statistics for analog distributed detection system when scale factor $\alpha = 1$. Since detection error probability in (3.23) increases as α decreases, it is easy to see that $\Sigma - \Delta$ modulation based system will outperform the analog system when $\alpha < 1$, i.e. $s^2/2 + \sigma_w^2 > 1$.

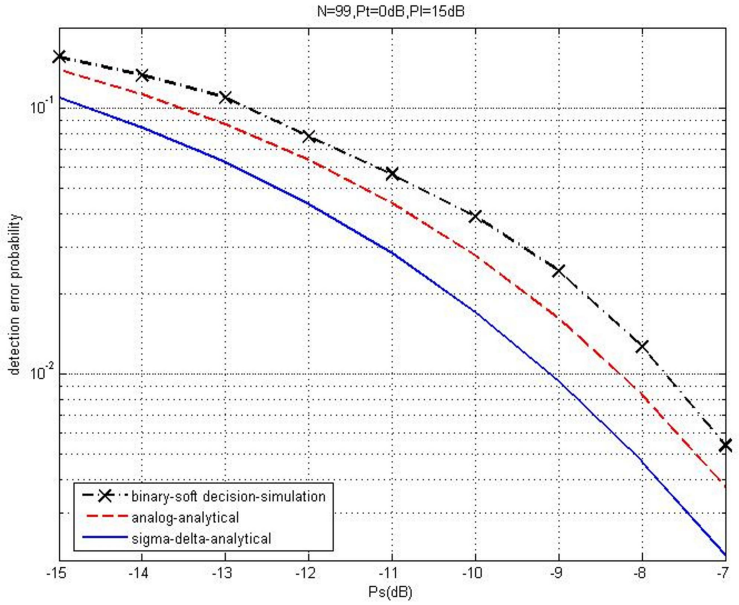

FIGURE 3.6. Detection error probability versus P_s in AWGN channels with N=99, P_t=0dB, P_I=15dB, s=0.6

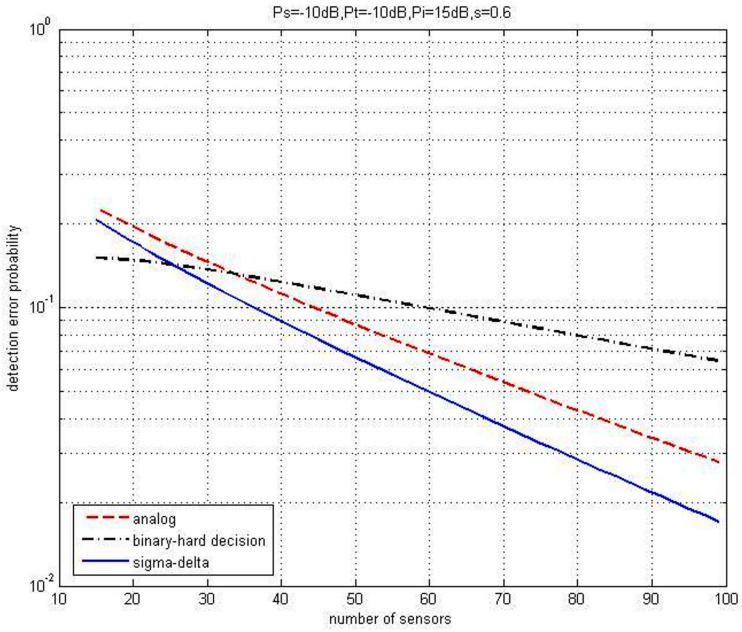

FIGURE 3.7. Detection error probability versus sensor number N in AWGN channels, P_I=15dB, P_t=10dB, P_s=10dB,s=0.6

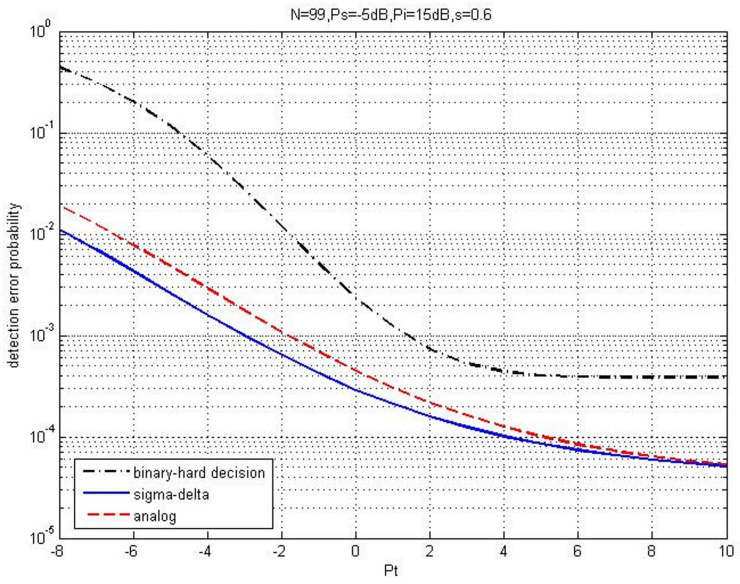

FIGURE 3.8. Detection error probability versus P_t in AWGN channel, P_s=-5dB, P_I=15dB, s=0.6, N=99

Summary

In this chapter, we

- Present the system model of distributed detection in AWGN channels.
- Investigate the statistical characteristics of the $\Sigma - \Delta$ modulation based on which we develop a suboptimal detector for $\Sigma - \Delta$ modulation based distributed detection system with closed-form detection error probability.
- Provide the optimal fusion rule for analog and binary system and its system performance.
- Evaluate the proposed system detection performance in AWGN channels by comparing it to the analog and binary systems.

Chapter 4

$\Sigma - \Delta$ modulation based distributed detection in non-coherent fading channels

In this chapter we extend the study to $\Sigma - \Delta$ modulation based distributed detection from AWGN channels to fading channels. For non-coherent detection in fading channels, it is generally impossible to obtain a closed-form formula for the detection error probability with finite number of sensors. We will provide the optimal fusion rule based on the joint pdf of $\{\hat{y}_i\}_{i=1}^N$ for the three distributed detection systems and evaluate their performances by simulations. We also study the alternative suboptimal detection algorithms for $\Sigma - \Delta$ modulation based system in order to gain some analytical insights.

4.1 System model

The distributed detection system model is similar to that described in section (3.1) except that, y_i is now transmitted to a fusion center respectively over a unique assigned channel that experiences independent flat fading with respect to other orthogonal channels. The received signal at the fusion center from the ith sensor node over fading channel now is

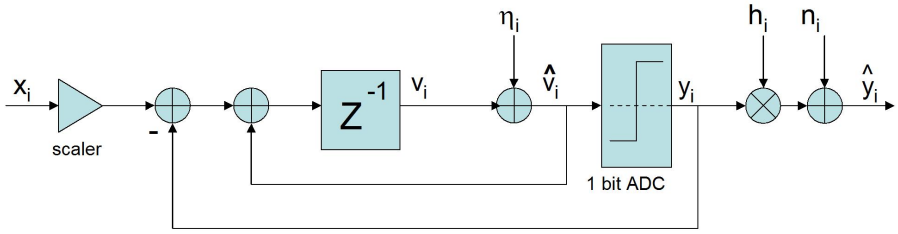

FIGURE 4.1. Equivalent model for $\Sigma - \Delta$ modulation based distributed detection system over fading channels

given by

$$\hat{y}_i = h_i y_i + n_i \tag{4.1}$$

where n_i is AWGN with variance σ_n^2 and h_i is the Rayleigh distributed fading channel gain with power $E(|h_i|^2) = 1$. The pdf of h_i is given by,

$$f(h_i) = 2h_i e^{-h_i^2}$$

We also assume non-coherent detection at fusion center where only channel fading statistics instead of global channel state information (CSI) is available. An equivalent system block diagram is shown in Fig. 4.1.

4.2 Iterative procedure to obtain joint pdf of $\Sigma - \Delta$ modulator output

In order to obtain the likelihood ratio in (1.2), we first need to get the joint pdf of $\{y_i\}_{i=1}^N$ at the $\Sigma-\Delta$ modulator output. [26] presents an iterative procedure to compute $f(y_1, \cdots, y_N)$. We will adopt this method and modify the algorithm to include the inter-sensor channel. Rewrite (3.11) we get,

$$v_{i+1} = x_i - e_i \tag{4.2}$$

where

$$e_i = q(\tilde{v}_i) - \tilde{v}_i \tag{4.3}$$

is the 1-bit quantization error and

$$\tilde{v}_i = v_i + \eta_i \tag{4.4}$$

is the received signal at sensor i from the previous sensor. Assuming that the stochastic process x_i and $-e(i)$ are independent, the pdf of v_{i+1} denoted as $f(v_{i+1})$ can be found as a convolution between the pdf of x_i and the reflected pdf of e_i denoted as $f(-e_i)$.

$$f(v_{i+1}) = f(x_i) * f(-e_i) \tag{4.5}$$

where the pdf of $-e_i$ follows from (4.3) as

$$f(-e_i = \nu) = u(\nu + 1)f(\tilde{v}_i = \nu) + u(-\nu + 1)f(\tilde{v}_i = \nu) \tag{4.6}$$

in which $u(e)$ is the step function defined as 0 for $e < 0$ and 1 for $e \geq 0$ and the pdf of $\tilde{v}_i$ follows from (4.4) as

$$f(\tilde{v}_i) = f(v_i) * f(\eta_i) \tag{4.7}$$

where $f(\eta_i)$ is a zero mean Gaussian pdf with variance σ_η^2. In order to find the pdfs $f(v_i)$ and $f(e_i)$ for every i, an initial value $v_1 = x_1 = m + w_1$ corresponding to a pdf with mean m and variance σ_w^2, and the initial quantization error pdf can be found by using (4.6) and (4.7). The procedure continues iteratively by finding the pdf of v_{i+1} with (4.5) where $f(x_i)$ is always a Gaussian pdf with mean m and variance σ_w^2. The actual calculation of these continuous pdfs requires a numerical evaluation and the accuracy of the algorithm depends on the resolution of the numerical convolution. The joint probability mass function (pmf) can thus by calculated by

$$P(y_1 = 1, \cdots, y_N = 1) = \int_0^\infty \cdots \int_0^\infty f(v_1, \cdots, v_N) dv_1 \cdots dv_N \tag{4.8}$$

4.3 LRT-based fusion algorithm for $\Sigma - \Delta$ modulation based distributed detection system

A straightforward approach to get $f(\hat{y}_1, \cdots, \hat{y}_N | H_j)$ for LRT rule is to write it as,

$$f(\hat{y}_1, \cdots, \hat{y}_N | H_j) = \sum_{y_1, \cdots, y_N} \prod_{i=1}^{N} f(\hat{y}_i | y_i) P(y_1, \cdots, y_N | H_j)$$

where $P(y_1, \cdots, y_N | H_j)$ can be numerically calculated using (4.8). However, this approach requires to sum up 2^N $P(y_1, \cdots, y_N | H_j)$, which means a computational complexity of $O(2^N)$. Instead we develop an iterative procedure to derive the desired joint pdf which only requires a computational complexity of $O(N)$.The algorithm will be referred as SLRT

(suboptimal LRT based) algorithm since we use approximation in the computing process and it is not the optimal way for calculating the LRT. First derive $f(\hat{y}_1, \cdots, \hat{y}_N|H_j)$ as,

$$\begin{aligned} f(\hat{y}_1, \cdots, \hat{y}_N|H_j) &= \prod_{i=2}^{N} f(\hat{y}_i|\hat{y}_{i-1}, \cdots, \hat{y}_1, H_j) f(\hat{y}_1|H_j) \\ &= \prod_{i=2}^{N} [\sum_{y_i} f(\hat{y}_i|y_i) P(y_i|\hat{y}_{i-1}, \cdots, \hat{y}_1, H_j)] f(\hat{y}_1|H_j) \\ &= \prod_{i=2}^{N} [\sum_{y_i} f(\hat{y}_i|y_i) P(y_i|\hat{y}_{i-1}, \cdots, \hat{y}_1, H_j)] \sum_{y_1} f(\hat{y}_1|y_1) P(y_1|H_j) \end{aligned} \tag{4.9}$$

Our algorithm is developed based on (4.9) to compute $f(\hat{y}_i|\hat{y}_{i-1}, \cdots, \hat{y}_1, H_j)$ for every i, which relies on the computation of $f(\hat{y}_i|y_i)$ and $P(y_i|\hat{y}_{i-1}, \cdots, \hat{y}_1, H_j)$ in each iteration. The details of each computation will be elaborated as follows.

First of all, $f(\hat{y}_i|y_i = 1)$ can be found as the convolution of the pdf of Gaussian zero-mean random variable n_i with variance σ_n^2 and the pdf of Rayleigh distributed random variable h_i with $E(h_i^2) = 1$. This pdf has a closed form derived as,

$$\begin{aligned} f(\hat{y}_i|y_i = 1) &= \int_0^\infty 2x e^{-x^2} \frac{1}{\sqrt{2\pi}\sigma_n} e^{-\frac{(x-y)^2}{2\sigma_n{}^2}} dx \\ &= \frac{2\sigma_n}{\sqrt{2\pi}(1+2\sigma_n^2)} e^{-\frac{y^2}{2\sigma_n^2}} [1 + \sqrt{2\pi} a y e^{\frac{(ay)^2}{2}} Q(-ay)] \end{aligned} \tag{4.10}$$

where

$$a = 1/(\sigma_n \sqrt{(1+2\sigma_n^2)}$$

Similarly we can find

$$f(\hat{y}_i|y_i = -1) = f(-\hat{y}_i|y_i = 1)$$

From Bayes rule, we can write

$$\frac{P(y_i = 1|\hat{y}_i)}{P(y_i = -1|\hat{y}_i)} = \frac{f(\hat{y}_i|y_i = 1)P(y_i = 1)}{f(\hat{y}_i|y_i = -1)P(y_i = -1)} \tag{4.11}$$

Here we assume the marginal probability of y_i without any condition $P(y_i = 1) = P(y_i = -1)$. Therefore, we can get $P(y_i|\hat{i})$ from (4.11) and the condition $P(yi = 1|\hat{i}) + P(yi = -1|\hat{i}) = 1$.

Secondly, the computation of $P(y_i|\hat{y}_{i-1},\cdots,\hat{y}_1,H_j)$ requires $f(v_i|\hat{y}_{i-1},\cdots,\hat{y}_1,H_j)$, for which we need to compute $f(v_{i-1}|\hat{y}_{i-1},\cdots,\hat{y}_1,H_j)$ first. for $f(v_{i-1}|\hat{y}_{i-1},\cdots,\hat{y}_1,H_j)$, we here use an approximation

$$f(v_{i-1}|\hat{y}_{i-1},\cdots,\hat{y}_1,H_j) = Norm[u(v_{i-1})f(v_{i-1}|\hat{y}_{i-2},\cdots,\hat{y}_1,H_j)]P(y_{i-1}=1|\hat{y}_{i-1})$$
$$+Norm[u(-v_{i-1})f(v_{i-1}|\hat{y}_{i-2},\cdots,\hat{y}_1,H_j)]P(y_{i-1}=-1|\hat{y}_{i-1}) \quad (4.12)$$

where $Norm(f(x)) = \frac{f(x)}{\int_{-\infty}^{\infty} f(x)dx}$ performs the normalization, $u(x)$ is the step function, $f(v_{i-1}|\hat{y}_{i-1},\cdots,\hat{y}_1,H_j)$ is obtained from the previous iteration and $P(yi-1|i\hat{-}1)$ can be computed using (4.11). In (4.12) we use a heuristic approach rather than the rigorous method using Bayes' rule. The idea is utilizing the updated $\hat{y}_{i-1}$ and the corresponding $P(y_{i-1}|\hat{y}_{i-1})$ in the $i-1$th iteration to reshape the conditional pdf of v_{i-1} given $\{\hat{y}_{i-2},\cdots,\hat{y}_1,Hj\}$, obtained from the $i-2$th iteration, which is simply scaled for positive v_{i-1} and negative v_{i-1} separately to get a heuristic $f(v_{i-1}|\hat{y}_{2-1},\cdots,\hat{y}_1,H_j)$.

The next step is to compute $f(v_i|\hat{y}_{i-1},\cdots,\hat{y}_1,H_j)$ based on $f(v_{i-1}|\hat{y}_{i-1},\cdots,\hat{y}_1,H_j)$ by applying the results in Section 4.2. Since

$$\begin{aligned} v_i &= x_i - e_{i-1} \quad (4.13)\\ &= x_i + \tilde{v}_{i-1} - q(\tilde{v}_{i-1}) \\ &= x_i + v_{i-1} + \eta_{i-1} - q(v_{i-1}+\eta_{i-1}) \end{aligned}$$

where e_i and $\tilde{v}_i$ are specified in (4.3) and (4.4). We first use $f(v_{i-1}|\hat{y}_{i-1},\cdots,\hat{y}_1,H_j)$ to get $f(\tilde{v}_{i-1}|\hat{y}_{i-2},\cdots,\hat{y}_1,H_j)$ and $f(-e_{i-1}|\hat{y}_{i-2},\cdots,\hat{y}_1,H_j)$ based on (4.3) and (4.4),

$$f(\tilde{v}_{i-1}|\hat{y}_{i-1},\cdots,\hat{y}_1,H_j) = f(v_{i-1}|\hat{y}_{i-1},\cdots,\hat{y}_1,H_j) * f(\eta_{i-1})$$

$$f(-e_{i-1}=\nu|\hat{y}_{i-1},\cdots,\hat{y}_1,H_j) =$$
$$u(\nu+1)f(\tilde{v}_{i-1}=\nu|\hat{y}_{i-1},\cdots,\hat{y}_1,H_j) + u(-\nu+1)f(\tilde{v}_{i-1}=\nu|\hat{y}_{i-1},\cdots,\hat{y}_1,H_j)$$

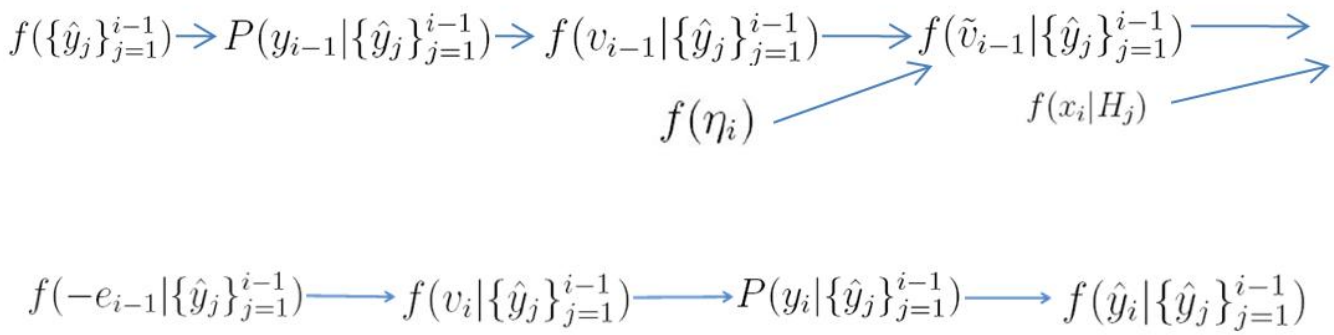

FIGURE 4.2. Iterative computation flow to calculate $f(\hat{y}_1, \cdots, \hat{y}_N|H_j)$

Then we can compute the desired $f(v_i|\hat{y}_{i-1}, \cdots, \hat{y}_1, H_j)$ using (4.13) as

$$f(v_i|\hat{y}_{i-1}, \cdots, \hat{y}_1, H_j) = f(x_i|H_j) * f(-e_{i-1}|\hat{y}_{i-1}, \cdots, \hat{y}_1, H_j)$$

and finally we can obtain $P(y_i|\hat{y}_{i-1}, \cdots, \hat{y}_1, H_j)$ as

$$P(y_i = 1|\hat{y}_{i-1}, \cdots, \hat{y}_1, H_j) = \int_0^\infty f(v_i|\hat{y}_{i-1}, \cdots, \hat{y}_1, H_j)dv_i$$

Using $P(y_i|\hat{y}_{i-1}, \cdots, \hat{y}_1, H_j)$ and $f(\hat{y}_i|y_i)$ computed for each i we can get the joint pdf of the received signals $f(\hat{y}_1, \cdots, \hat{y}_N|H_j)$ under each hypothesis using (4.9). Note that initial value $v_1 = x_1 + \eta_1$, corresponding a Gaussian distributed pdf with mean m and variance $\sigma_w^2 + \sigma_\eta^2$ and $P(y_1 = 1|H_j) = \int_0^\infty f(v_1|H_j)dv_1$.

The essence of the algorithm lies in the prediction of the pdf of $\hat{y}_i$ given $\{\hat{y}_j\}_{j=1}^{i-1}$. The computation process flows as $f(\{\hat{y}_j\}_{j=1}^{i-1})$, $P(y_{i-1}|\{\hat{y}_j\}_{j=1}^{i-1})$, $f(v_{i-1}|\{\hat{y}_j\}_{j=1}^{i-1})$, $f(\tilde{v}_{i-1}|\{\hat{y}_j\}_{j=1}^{i-1})$, $f(-e_{i-1}|\{\hat{y}_j\}_{j=1}^{i-1})$, $f(v_i|\{\hat{y}_j\}_{j=1}^{i-1})$, $P(y_i|\{\hat{y}_j\}_{j=1}^{i-1})$, $f(\hat{y}_i|\{\hat{y}_j\}_{j=1}^{i-1})$, as illustrated in Fig 4.2. The procedure continues N times and the likelihood ratio of the received $\{\hat{y}_i\}_{i=1}^N$ can hence be numerically computed. The SLRT detector is thus constructed straightforwardly.

As an alternative approach, EGC is adopted again as suboptimal detector. EGC for distributed detection over fading channels will be analyzed in Section 5.1. Due to the fading gain h_i, EGC can no longer eliminate the quantization noise power as in AWGN

case, its usefulness yet depends on how much performance loss it suffered compared to the optimal fusion rule. In the context of non-coherent fading detection, it is the only suboptimal detector that do not need global CSI.

4.4 Optimal fusion rule for Binary and Analog distributed detection system

Similar to the distributed detection over AWGN channels, we also need to develop optimal detectors for binary and analog systems to compare their detection performance.

Binary case:

For binary distributed detection system over fading channel, the local sensor has the same decision threshold $s/2$ as the AWGN case. The desired LR at the fusion center is

$$\Lambda = \prod_{i=1}^{N} \frac{P_f f(\hat{y}_i|y_i = 1) + (1 - P_f) f(\hat{y}_i|y_i = -1)}{P_f f(\hat{y}_i|y_i = -1) + (1 - P_f) f(\hat{y}_i|y_i = 1)}$$

where $f(\hat{y}_i|y_i = 1)$ is specified in (4.10) and $P_f = Q(s/2\sigma_w)$.

Analog case:

For analog system, $y_i = \alpha x_i$, the breceived signal at the fusion center $\hat{y}_i$ is

$$\hat{y}_i = h_i \alpha (m + w_i) + n_i$$

Conditional on h_i $\hat{y}_i$ is a Gaussian distributed random variable with mean $h_i \alpha m$ and variance $h_i^2 \alpha^2 \sigma_w^2 + \sigma_n^2$, the joint pdf of $\{\hat{y}_i\}_{i=1}^N$ can be obtained by

$$f(\hat{y}_1, \cdots, \hat{y}_N|H_j) = \prod_{i=1}^{N} \int_0^\infty f(\hat{y}_i|h_i, H_j) f(h_i) dh_i$$

$$= \prod_{i=1}^{N} \int_0^\infty 2h e^{-h^2} \frac{1}{\sqrt{2\pi(h^2\alpha^2\sigma_w^2 + \sigma_n^2)}} e^{-\frac{(\hat{y}_i - \alpha h m)^2}{(h^2\alpha^2\sigma_w^2 + \sigma_n^2)}} dh$$

The rest of the procedure to obtain the LR is exactly the same as the binary case. The comparison between the three schemes will be discussed in Section. 4.5.

4.5 Performance evaluation

We investigate the detection performance of $\Sigma-\Delta$ modulation based distributed detection using the SLRT algorithm with respect to various parameters, under the 1st order Markov process approximation of $\{\hat{y}_{i=1}^{N}\}$, compared to the performance of analog, binary system as well as suboptimal EGC detector of $\Sigma-\Delta$. Benchmark curve of optimal detection performance without any channel distortion is also shown. As illustrated by Fig. 4.5, $\Sigma-\Delta$ performance is a convex function of s with optimal value around 0.8. The sensor node should scale input signal first or choose the proper quantization level of the 1 bit quantizer to achieve the optimal performance. Clearly $\Sigma-\Delta$ distributed detection system with SLRT detector can outperform both analog and binary sensor nodes with the extra links between sensor nodes and it can be very robust against the fading channel distortion with performance very close to the optimal detection assuming input signal is directly accessible to the fusion center, as evidenced by Fig. 4.3 and Fig. 4.4. The question is how much performance degrading will the inter-sensor channel distortion cause on the overall performance of the system.

Our study in $\Sigma-\Delta$ modulation based distributed detection assumes that there is no fading in the inter-sensor channels. It is reasonable because of the close distance between adjacent sensor nodes. However, we would like to see how much our proposed system will suffer if there is also fading effect existing in the inter-sensor channels. Fig. 4.6 provided the detection performance of $\Sigma-\Delta$ system as a function of P_I with both fading inter-sensor channel and non-fading inter-sensor channel being examined. It demonstrates that for non-fading inter-sensor channels, we need at least $10dB$ inter-sensor channel SNR to assure the performance advantage. For fading inter-sensor channel case, we still use the fusion rule assuming the inter-sensor channel is AWGN. The received signal from the ith sensor at the $i+1$th sensor becomes

$$\hat{v}_i = \bar{h}_i v_i + \eta_i$$

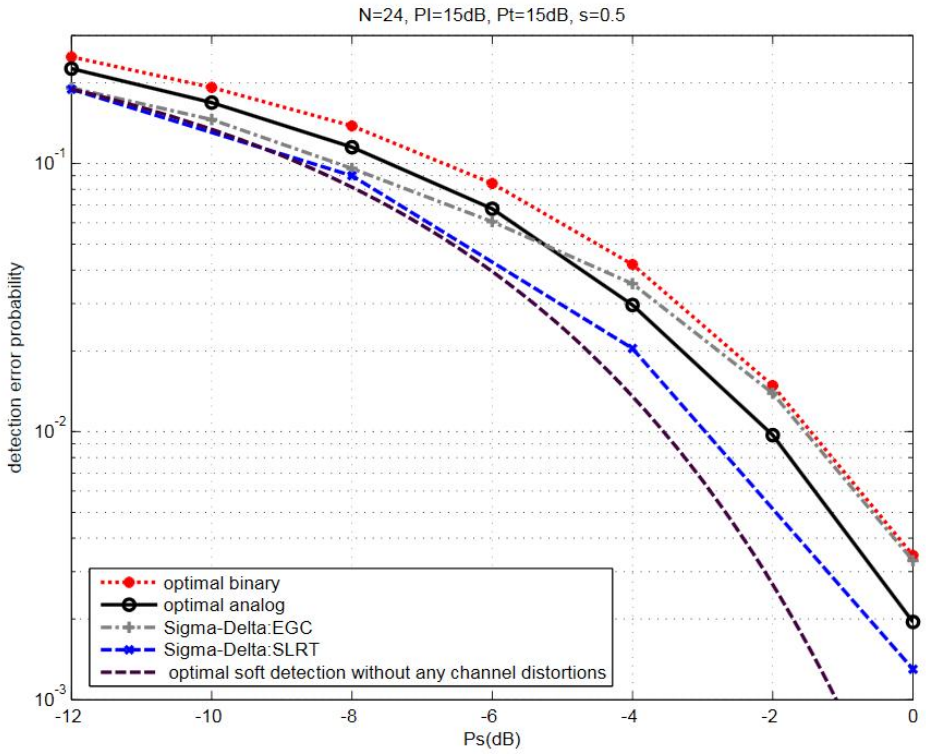

FIGURE 4.3. Noncoherent detection error probability versus P_s, P_I=15dB, P_t=15dB, s=0.5, N=24

where $\bar{h}_i$ is the Rayleigh distributed fading gain with $E(\bar{h}_i^2) = 1$ and η_i is the inter-sensor channel white Gaussian noise. From the simulation results, the detection performance degrades substantially. This illustrates that the $\Sigma - \Delta$ modulation based distributed detection needs reliable inter-sensor communication to achieve its potential benefits since it requires additional communication links between local sensor nodes.

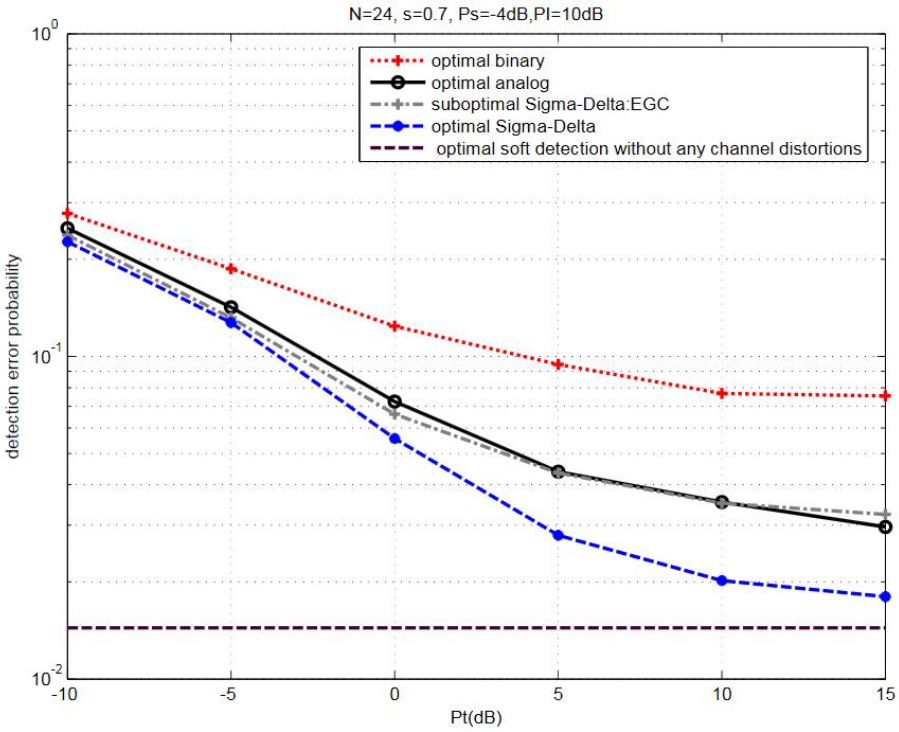

FIGURE 4.4. Noncoherent detection error probability versus P_t, P_I=15dB, P_s=-4dB, s=0.7, N=24

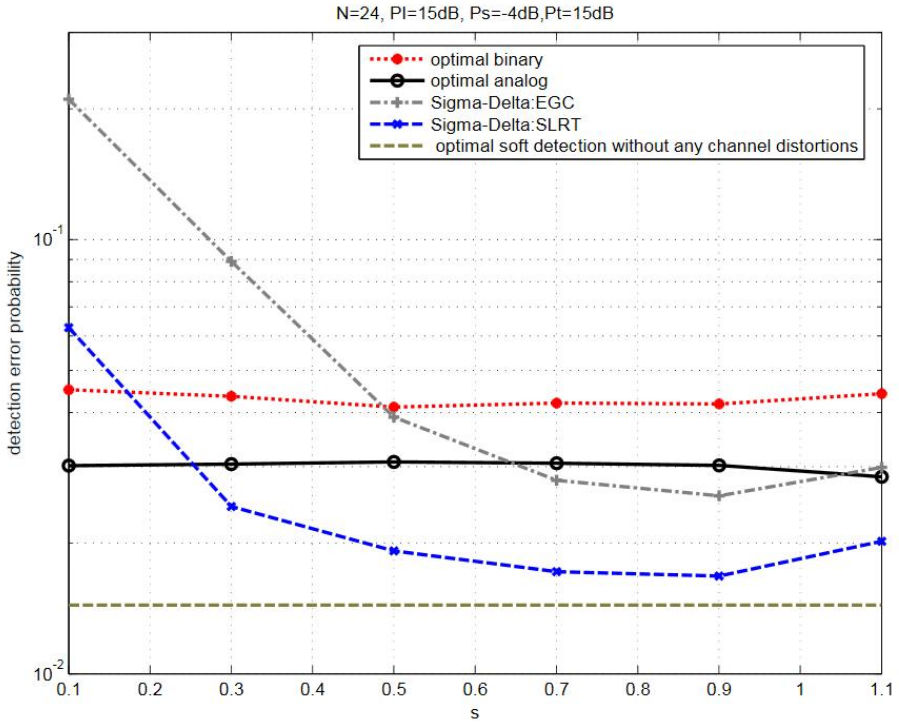

FIGURE 4.5. Noncoherent detection error probability versus s, P_s=-4dB, P_I=15dB, P_t=15dB, N=24

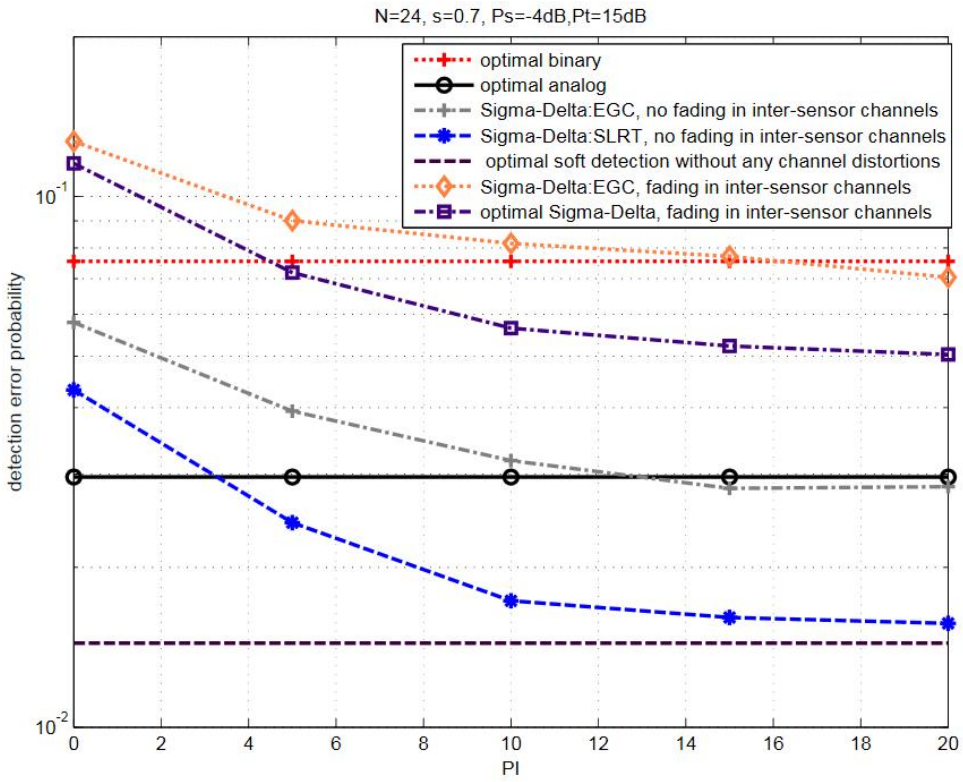

FIGURE 4.6. Noncoherent detection error probability versus P_I, P_s=-4dB, P_t=15dB, s=0.7, N=24

Summary

In this chapter, we

- Investigate the distributed detection system in non-coherent fading channels.
- Develop the optimal fusion algorithm for $\Sigma-\Delta$ modulation based distributed detection system.
- Provide the optimal fusion rule for analog and binary systems in non-coherent fading channels.
- Evaluate the proposed system performance in non-coherent fading channels by comparing it to the analog and binary systems.

Chapter 5

Distributed detection of correlated observations over coherent fading channels

Although the reliance on the global Channel State Information (CSI) in obtaining the local decision rules was relaxed to make the distribute detection system more practical, in certain applications we may still be able to afford obtaining the complete knowledge of CSI through training-based channel estimation for slowly varying channels. Thus the distributed detection with coherent reception will be studied in order to see how much we can gain by obtaining CSI in terms of detection performance. In this chapter, we will provide more thorough comparison between different schemes, based on the analysis of their asymptotical performance in high P_t and P_s region. Furthermore, we would like to see what effect would be caused on the detection performance of distributed detection when the observations at local sensor nodes are correlated.

5.1 Fusion rules for distributed detection over coherent fading channels

From the numerical results of performance discrepancy between binary and analog distributed detection system in AWGN channels, we know that under different channel and sensor conditions, the performance comparison exhibits different behaviors. To be specific, analog system has stronger performance in low P_s region and high P_t region, and binary system outperforms analog system in low P_t region and high P_s region. We try to see this result can be duplicated in fading channels. What's more, we will also investigate the performance of our proposed $\Sigma - \Delta$ distributed detection system in coherent fading channels.

Binary system

In binary distributed detection systems, local optimal binary decision is still made in each sensor node by comparing the measurement x_i with the threshold of $s/2$ and then transmits

the binary message to the fusion center. Given the transmitted signal, the received signal from the ith sensor node becomes a Gaussian random variable with mean $\pm h_i$ and variance σ_n^2. The LR of $\{\hat{y}_i\}_{i=1}^N$ given $\{h_i\}_{i=1}^N$ at the fusion center under two hypothesis can be modified from (3.21),

$$\begin{aligned}\Lambda &= \prod_{i=1}^{N} \frac{f(y_i|H_0,h_i)}{f(y_i|H_1,h_i)} \\ &= \prod_{i=1}^{N} \frac{P_f e^{-\frac{(\hat{y}_i-h_i)^2}{2\sigma_n^2}} + (1-P_f)e^{-\frac{(\hat{y}_i+h_i)^2}{2\sigma_n^2}}}{P_f e^{-\frac{(\hat{y}_i+h_i)}{2\sigma_n^2}} + (1-P_f)e^{-\frac{(\hat{y}_i-h_i)}{2\sigma_n^2}}}\end{aligned} \tag{5.1}$$

where $P_f = Q(s/2\sigma_w)$. The optimal detection employing the LRT based fusion rule can then be constructed.

Analog system

For analog system, each sensor node scales the local observation x_i by a factor of $\alpha = \sqrt{\frac{2}{s^2+2\sigma_w^2}}$ and transmits to the fusion center through the coherent fading channel. The received signal from the ith sensor node becomes a Gaussian random variable with mean $\alpha h_i m$ and variance $\alpha^2 h_i^2 \sigma_w^2 + \sigma_n^2$. The LR of $\{\hat{y}_i\}_{i=1}^N$ given $\{h_i\}_{i=1}^N$ at the fusion center under two hypothesis can be written as

$$\begin{aligned}\Lambda &= \prod_{i=1}^{N} \frac{f(y_i|H_0,h_i)}{f(y_i|H_1,h_i)} \\ &= \prod_{i=1}^{N} \frac{e^{-\frac{(\hat{y}_i)^2}{2\alpha^2 h_i^2 \sigma_w^2+\sigma_n^2}}}{e^{-\frac{(\hat{y}_i-\alpha h_i s)^2}{2\alpha^2 h_i^2 \sigma_w^2+\sigma_n^2}}}\end{aligned} \tag{5.2}$$

The optimal LRT based fusion rule for analog distributed detection system can be implemented exactly like the previous cases.

$\Sigma-\Delta$ modulation based system

The joint pdf of received signals $\{\hat{y}_i\}_{i=1}^N$ for $\Sigma-\Delta$ modulation based distributed detection system can be derived similar as (4.9) except that the channel condition is changed because

of CSI.

$$
\begin{aligned}
& f(\hat{y}_1, \cdots, \hat{y}_N | H_j, h_1, \cdots, h_N) \\
&= \prod_{i=2}^{N} f(\hat{y}_i | \hat{y}_{i-1}, \cdots, \hat{y}_1, H_j, h_{i-1}, \cdots, h_1) f(\hat{y}_1 | H_j, h_1) \\
&= \prod_{i=2}^{N} [\sum_{y_i} f(\hat{y}_i | y_i, h_i) P(y_i | \hat{y}_{i-1}, \cdots, \hat{y}_1, H_j, h_{i-1}, \cdots, h_1)] f(\hat{y}_1 | H_j, h_1)
\end{aligned}
$$

where

$$
f(\hat{y}_i | y_i, h_i) = \frac{1}{\sqrt{2\pi}\sigma_n} e^{-\frac{(\hat{y}_i - h_i y_i)^2}{2\sigma_n^2}}
$$

and

$$
\frac{P(y_i = 1 | \hat{y}_i, h_i)}{P(y_i = -1 | \hat{y}_i, h_i)} = \frac{f(\hat{y}_i | y_i = 1, h_i) f(y_i = 1, h_i)}{f(\hat{y}_i | y_i = -1, h_i) f(y_i = -1, h_i)}
$$

. we use the similar assumption $f(y_i = 1, h_i) = f(y_i = -1, h_i)$ so that $P(y_i = 1 | \hat{y}_i, h_i)$ can be computed. The rest of the steps to find $P(y_i | \hat{y}_{i-1}, \cdots, \hat{y}_1, H_j, h_{i-1}, \cdots, h_1)$ are similar to those in section 4.3.

The LRT based fusion rule can now be implemented using the SLRT algorithm. Like AWGN and non-coherent fading case, we would like to investigate alternative suboptimal fusion rule to gain more insights. EGC has been shown to be an efficient suboptimal detector for $\Sigma - \Delta$ modulation based distributed detection systems. There are some other suboptimal detector for coherent detection. For coherent fading channels, maximum ratio combining is known as a diversity technique that achieves maximum SNR in wireless communications [29]. It is one of the best techniques to mitigate the effect of fading in diversity combining of independently fading signal paths. Applying this technique in distributed

detection, we modify the detection statistics in (3.15) to,

$$\begin{aligned} Z_{MRC} &= \frac{1}{N}\sum_{i=1}^{N} h_i \hat{y}_i \\ &= \frac{1}{N}\sum_{i=1}^{N} h_i (h_i y_i + n_i) \\ &= \frac{1}{N}\sum_{i=1}^{N} [h_i^2 (m + w_i + \eta_i) + h_i n_i + h_i^2 (\bar{e}_i - \bar{e}_{i+1})] \end{aligned} \tag{5.3}$$

while the detection statistics for EGC without the requirement of channel CSI is

$$\begin{aligned} Z_{EGC} &= \frac{1}{N}\sum_{i=1}^{N} \hat{y}_i \\ &= \frac{1}{N}\sum_{i=1}^{N} (h_i y_i + n_i) \\ &= \frac{1}{N}\sum_{i=1}^{N} [h_i (m + w_i + \eta_i) + n_i + h_i (\bar{e}_i - \bar{e}_{i+1})] \end{aligned} \tag{5.4}$$

While MRC is optimal in that in maximizes the output SNR in the communication link from local sensors to the fusion center, it does not deal with the sensor SNR. In the context of sensor networks, this is not necessarily the case due to the nature of the problem. To analyze this, based on (5.3) and (5.4) we can calculate the first two moments of the test statistics and write the detection-wise SNR by applying the Central Limit Theorem (CLT) and Gaussian approximation,

$$SNR_{MRC} = \frac{s^2}{\frac{1}{N}\{2(\sigma_w^2 + \sigma_\eta^2) + m^2 + \sigma_n^2 + 2E[(\bar{e}_i - \bar{e}_{i+1})^2]\}} \tag{5.5}$$

$$SNR_{EGC} = \frac{s^2}{\frac{1}{N}\frac{4}{\pi}\{\sigma_w^2 + \sigma_\eta^2 + (1 - \frac{\pi}{4})m^2 + \sigma_n^2 + E[(\bar{e}_i - \bar{e}_{i+1})^2]\}} \tag{5.6}$$

By comparing the denominators in (5.5) and (5.6), we find that MRC only maximize the signal to channel noise (n_i) ratio while EGC is more robust against all the other noise components (w_i, η_i, and $\bar{e}_i - \bar{e}_{i+1}$). Unless channel noise is overwhelming, EGC should be preferable since it requires least of the channel information, as evidenced by the simulation

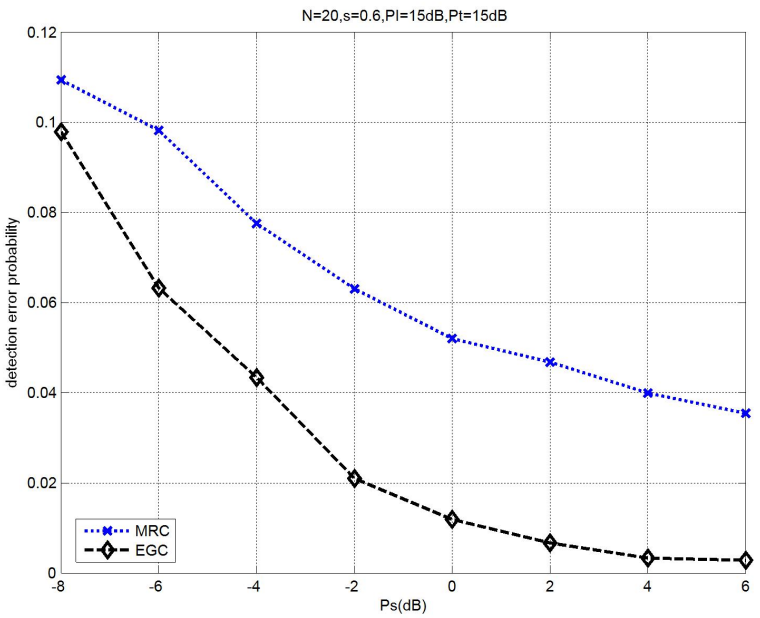

FIGURE 5.1. Simulation results of detection error probability versus Ps for MRC and EGC, Pt=15dB, PI=15dB, s=0.6, N=20

results given in Fig. 5.1, Fig. 5.2 and Fig. 5.3. We compare the detection performance of the two suboptimal fusion rule versus P_s for different channel SNR P_t. EGC outperforms MRC in all cases.

We approximate $E[(\bar{e}_i - \bar{e}_{i+1})^2] = 2/3 - 2R_{\bar{e}_i}(1)$ [23] and the detection error probability can be evaluated easily [28] applying Gaussian density function with obtained mean and variance. We compared this approximation to the simulation result of EGC.

Fig. 5.4 gives the detection error probability versus P_s obtained by simulation and analytical approximation using the CLT for EGC as a suboptimal detector. In this example, the total number of sensors is 15, P_I is $15dB$ and P_t is $10dB$. While some discrepancy exists, the approximation using the CLT matches relatively well to the simulation results in high sensor SNR region. We have also found through extensive simulations that the accuracy of the CLT approximation not only depends on P_s but also other parameters such as N, P_I and P_t.

Single sensor detection with binary repetition coding scheme

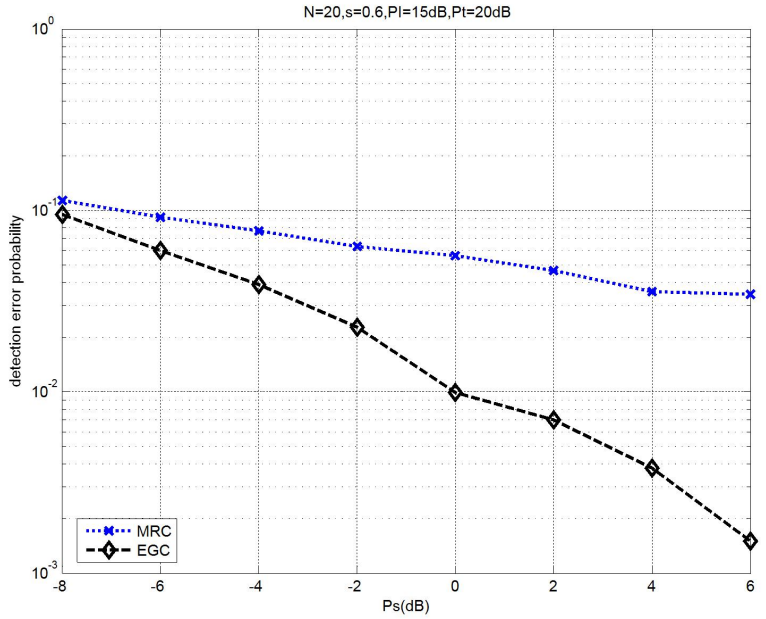

FIGURE 5.2. Simulation results of detection error probability versus Ps for MRC and EGC, Pt=20dB, PI=15dB, s=0.6, N=20

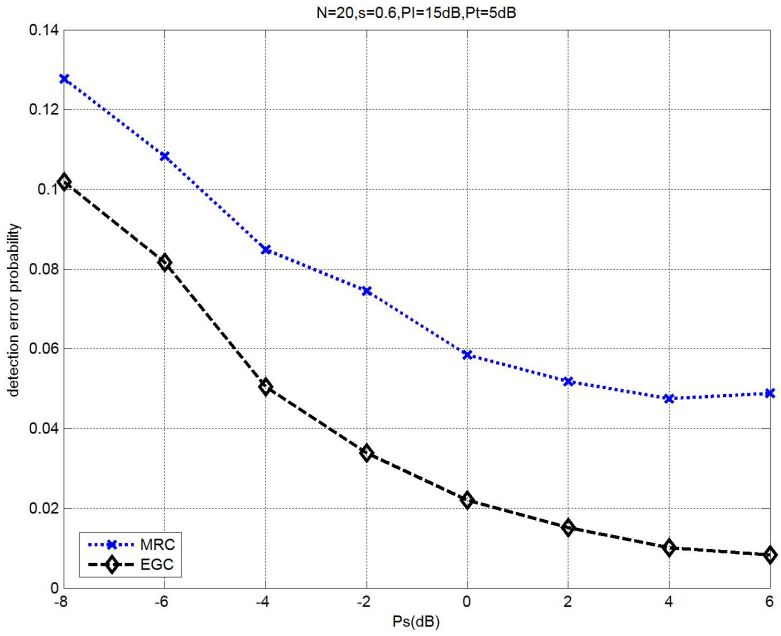

FIGURE 5.3. Simulation results of detection error probability versus Ps for MRC and EGC, Pt=5dB, PI=15dB, s=0.6, N=20

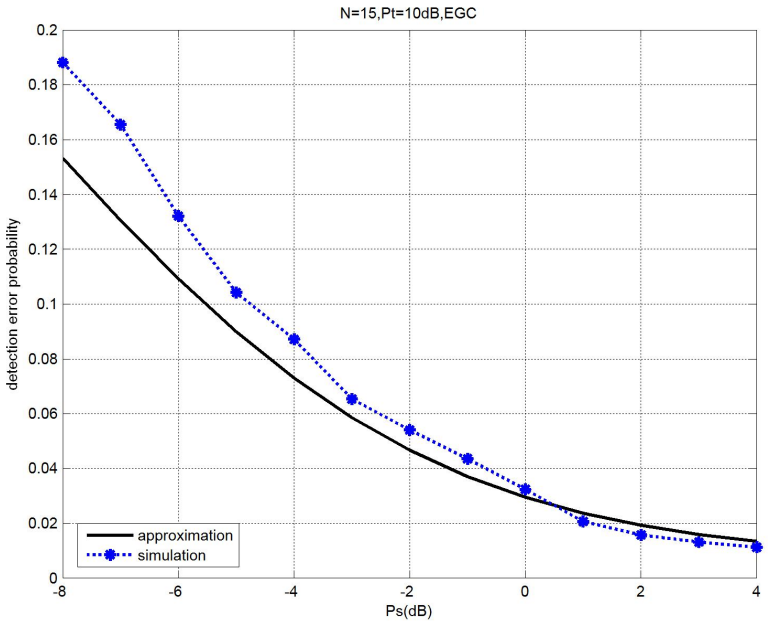

FIGURE 5.4. Detection error probability versus P_s obtained by simulation and numerical approximation for suboptimal detector EGC, P_t=10dB, N=15, P_I=15dB

In addition to these three schemes, consider a single binary sensor detection with K observations $\{x_1, x_2, \cdots, x_K\}$. It makes a local optimal decision y based on LRT of k samples and transmit the decision repeatedly L times (denoted as $\{y_1, y_2, \cdots, y_L\}$) to the fusion center.

For analytic purposes, assume the fusion center uses MRC to decide the local binary decision y and the hypothesis H_i upon receiving $\{\hat{y}_1, \hat{y}_2, \cdots, \hat{y}_L\}$. Specifically, the MRC decision rule at the fusion center,

$$R = \sum_{i=1}^{L} h_i \hat{y}_i$$

The signal to noise ratio of the output R is

$$\gamma_\Sigma = \Sigma_{i=1}^{L} \frac{h_i^2}{\sigma_n^2} = \Sigma_{i=1}^{L} h_i^2 P_t$$

Assume i.i.d. Rayleigh fading on each branch of MRC with equal average SNR $E(h_i^2)P_t = P_t$, the distribution of γ_Σ is χ^2 with $2L$ degrees of freedom,

$$p_{\gamma_\Sigma}(\gamma) = \frac{\gamma^{L-1} e^{-\gamma/P_t}}{P_t^L (L-1)!}, \quad \gamma \geq 0$$

The transmission error probability given global CSI $P(\hat{y} \neq y|h_1, \cdots, h_L)$ is given as

$$P(\hat{y} \neq y|h_1, \cdots, h_L) = Q(\sqrt{2\gamma_\Sigma})$$

where the decision rule is

$$\hat{y} = \begin{cases} 1, \ R \geq 0, \\ -1, \ R < 0. \end{cases}$$

The average probability of transmission error is

$$\begin{aligned} P_b &= P(\hat{y} \neq y) = \int_0^\infty Q(\sqrt{2\gamma_\Sigma}) p_{\gamma_\Sigma}(\gamma) d\gamma \\ &= (\frac{1-\Gamma}{2})^L \Sigma_{l=1}^{L-1} (\tbinom{L-1+l}{l}) (\frac{1+\Gamma}{2})^l, \end{aligned}$$

where $\Gamma = \sqrt{P_t/(1+P_t)}$. The total detection error probability for single binary sensor with K observations and L repetitions is,

$$\begin{aligned} P_{e,rep} &= P(\hat{y}=1|H_0)P(H_0) + P(\hat{y}=-1|H_1)P(H_1) \\ &= P(\hat{y}=1|y=1)P(y=1|H_0)P(H_0) + P(\hat{y}=1|y=-1)P(y=-1|H_0)P(H_0) \\ &+ P(\hat{y}=-1|y=1)P(y=1|H_1)P(H_1) + P(\hat{y}=-1|y=-1)P(y=-1|H_0)P(H_0) \\ &= P_f(1-P_b) + (1-P_f)P_b \end{aligned} \tag{5.7}$$

where $P_f = Q(\frac{s/2}{\sqrt{\sigma_n^2/K}})$ is the local detection error using K i.i.d. Gaussian observations. This equation is plotted in Fig. 5.5.

The relations between P_e and K, L, P_t, P_s depicted in Fig. 5.5 and Fig. 5.7 can be shown from (5.7). Assuming $K+L$ is constant, high P_t and low P_s results in that P_e is dominated by $P_f(1-P_b)$, which means larger K leads to overall better detection performance. On contrast, low P_t and high P_s results in that P_e is dominated by $(1-P_f)P_b$, and thus larger L is in favor of in this case. Although this is a single sensor detection scheme, we would like to see how well its performance is by comparing it to distributed detection systems with $K = L = N$.

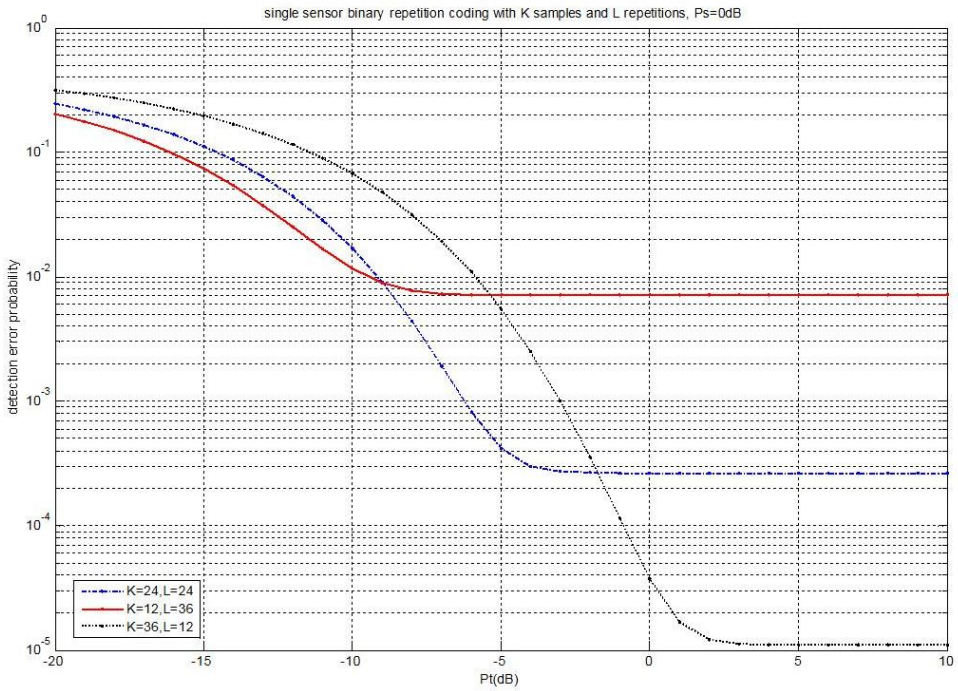

FIGURE 5.5. Detection error probability versus P_t of single binary sensor with repetition coding in coherent fading channels

5.1.1 Performance evaluation

The simulation results of comparison between single binary sensor detection with repetition coding, binary distributed system, analog distributed system and $\Sigma - \Delta$ distributed detection system in coherent fading channels are provided in Fig. 5.7 and Fig. 5.8, where $K = L = N = 24$ and observations are conditionally independent. Optimal detection rules are adopted for binary distributed system, analog distributed system and $\Sigma - \Delta$ distributed detection system using SLRT detection algorithm. Analytical results for binary repetition coding scheme is provided using (5.7).

First of all, these results shows that if the single sensor detection scheme can be implemented in the distributed detection framework, significant performance improvement can be achieved.

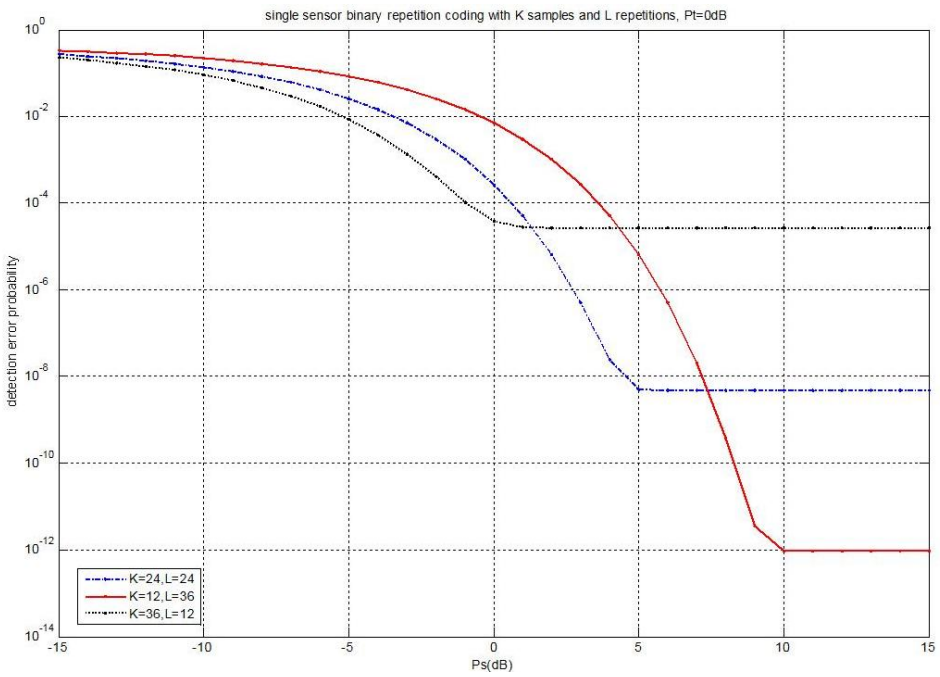

FIGURE 5.6. Detection error probability versus P_s of single binary sensor with repetition coding in coherent fading channels

To further understand the performance discrepancy of the other three distributed detection schemes. Asymptotical performance will be analyzed for different schemes with very large P_t and P_s, which is consistent with the error floors in the simulation results.

As P_t goes to infinity, analog system with fixed P_s renders the optimal performance of the scenario that all the observations are directly accessible to the fusion center,

$$P_{e,a,P_t\to\infty} = Q(\frac{s/2}{\sqrt{\sigma_w^2/N}}) \tag{5.8}$$

Same results can be justified for single binary sensor detection with repetition coding and $\Sigma-\Delta$ distributed system. For binary distributed detection system, as P_t increases to infinity, local binary decisions are available to the fusion center error free, and the LRT decision rule simplifies to the form of majority vote. The corresponding detection error probability is characterized by,

$$P_{e,b,P_t\to\infty} = \sum_{i=1}^{\lceil\frac{N}{2}\rceil}[1-Q(\frac{s/2}{\sigma_w})]^i[Q(\frac{s/2}{\sigma_w})]^{(N-i)}$$

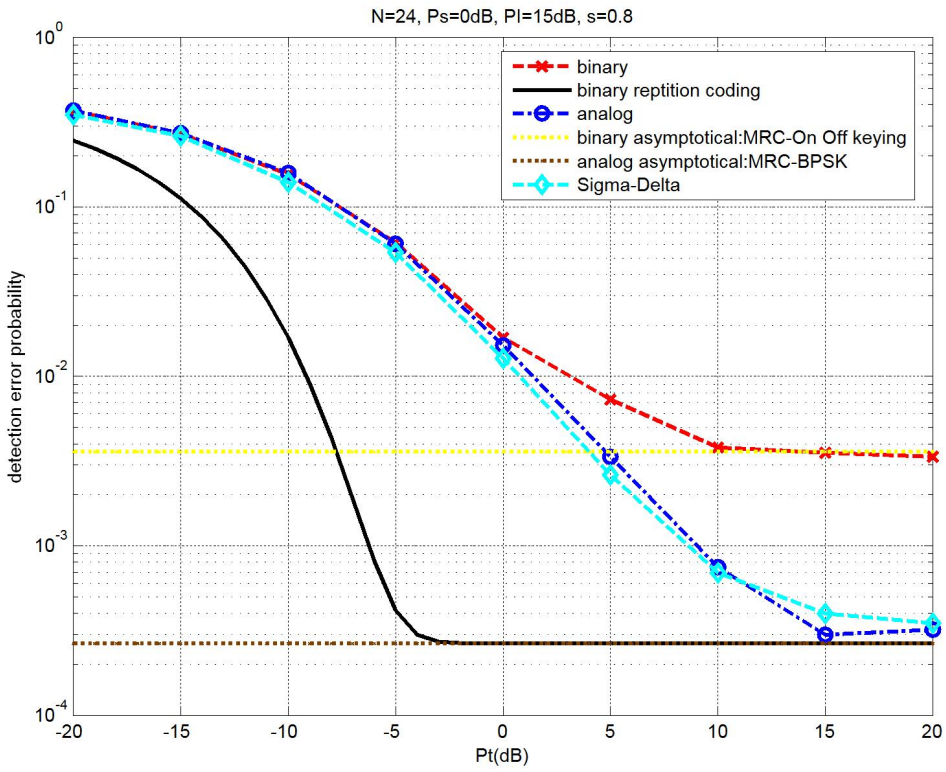

FIGURE 5.7. Detection performance comparison between single binary sensor with repetition coding, distributed binary sensors, distributed analog sensors and $\Sigma-\Delta$ distributed sensors using SLRT algorithm in coherent fading channels, K=L=N=24, P_e versus P_t

This error probability is larger than (5.8), which is shown in Fig. 5.7 as the gap between the error floors of analog and binary system.

On the other hand, as P_s increases to infinity, local observations are deterministic constant signal given the hypothesis and distributed detection becomes a pure communication problem. For binary distributed system, all the transmitted signal from local sensors are bit ones given H_1 and bit zeros given H_0. This is the same as the binary repetition coding scheme. The probability of error is reduced to the form of P_b in (5.7).

$$\begin{aligned} P_{e,b,P_s\to\infty} &= \int_0^\infty Q(\sqrt{2\gamma_\Sigma}) p_{\gamma_\Sigma}(\gamma) d\gamma \\ &= (\frac{1-\Gamma}{2})^L \Sigma_{l=1}^{L-1} \binom{L-1+l}{l} (\frac{1+\Gamma}{2})^l, \end{aligned}$$

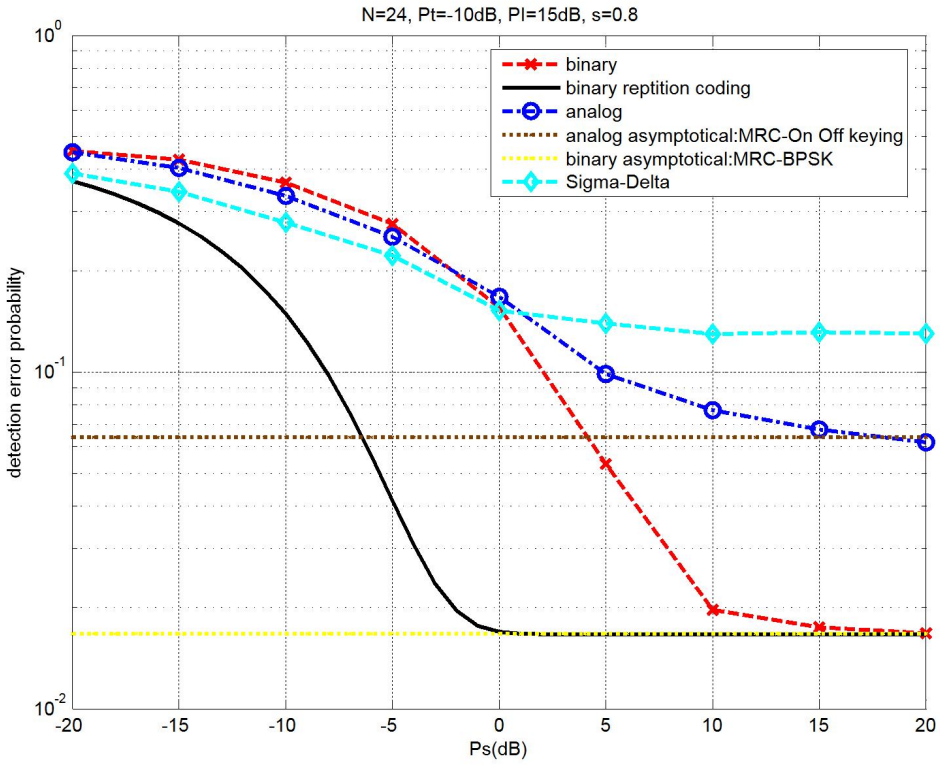

FIGURE 5.8. Detection performance comparison between single binary sensor with repetition coding, distributed binary sensors, distributed analog sensors and $\Sigma - \Delta$ distributed sensors using SLRT algorithm in coherent fading channels, K=L=N=24, P_e versus P_s

where $\Gamma = \sqrt{P_t/(1+P_t)}$. This is the average transmission error probability in coherent fading channels with BPSK modulation and N branch MRC.

For analog system, all the local sensors directly transmit the same signal αm to the fusion center. $\alpha m = \sqrt{2}$ given H_1 and $\alpha m = 0$ given H_0. This is equivalently the on-off keying modulation in digital communications. Using maximum ratio combing, the average error probability can be calculated by

$$P_{e,a,P_s\to\infty} = \int_0^\infty Q(\sqrt{\gamma_\Sigma}) p_{\gamma_\Sigma}(\gamma) d\gamma$$

Essentially for binary and analog distributed detection systems, the problem is simplified as transmitting a binary hypothesis with repetition coding schemes of length N. The difference between analog system and binary system in high P_s region is the values of the repetition code symbol, which can be considered as different digital modulation types equivalently. Since BPSK has larger Euclidean distance between two basis function than On-Off keying, the probability of error given channel CSI for binary system $Q(\sqrt{2\gamma_\Sigma})$ is smaller than that of analog system $Q(\sqrt{\gamma_\Sigma})$ given the same average transmission power, resulting in the overall detection performance difference illustrated in Fig. 5.7. For $\Sigma - \Delta$ distributed detection system, the transmitted sequence $\{y_i\}$ when $s = 1$ is $\{1, -1, 1, -1, \cdots\}$ given H_1 and $\{0, 0, \cdots\}$ given H_0 [21]. The Euclidean distance between the two codes is smaller than binary and analog system. Therefore, in high P_s region $\Sigma - \Delta$ scheme has the worst performance of all.

As for the case of low P_s and P_t region, the results shown in simulations are similar to AWGN and noncoherent fading cases as expected.

In summery, binary repetition coding scheme has the overall best performance. Among the other three distributed schemes,

- In high P_s region, binary system has the best performance of three.
- In high P_t region, analog system and $\Sigma - \Delta$ system has better performance than binary

system.

• In low P_s region, $\Sigma - \Delta$ system has the best performance of three. Analog system has better performance than binary system.

• In low P_t region, $\Sigma - \Delta$ system has the best performance of three. Binary system has better performance than analog system.

	Analog	Binary	Repetition Coding	$\Sigma - \Delta$
High P_t Region (Asymptotical)	Optimal	Majority vote	Optimal	Optimal
High P_s Region (Asymptotical)	MRC with On-Off Keying	MRC with BPSK	MRC with BPSK	Smallest distance
Low P_t Region	Worst	Third	Best	Second
Low P_s Region	Third	Worst	Best	Second

TABLE 1. Summary of detection performance of different schemes.

5.2 Detection of correlated observations

The distributed detection study presented in this thesis so far assumes that sensor observations are conditionally independent with the joint pdf of the observations obeys (1.3). Although this assumption is easy to analyze, there are many occasions where the observations at the different sensors consist of noisy observations of random signals which are correlated. We will provide an example of detecting correlated observations with corresponding fusion rules for different schemes in this section.

Assume the covariance matrix of the measurement noise w_i is

$$K_w = \begin{bmatrix} \sigma_w^2 & \sigma_w^2/2 & 0 & \cdots & \cdots & \cdots & 0 \\ \sigma_w^2/2 & \sigma_w^2 & \sigma_w^2/2 & 0 & \cdots & \cdots & 0 \\ 0 & \sigma_w^2/2 & \sigma_w^2 & \sigma_w^2/2 & & & \vdots \\ \vdots & \cdots & \cdots & \ddots & \ddots & & \vdots \\ 0 & 0 & \cdots & \cdots & \ddots & \ddots & \vdots \\ 0 & 0 & 0 & \cdots & \cdots & \sigma_w^2 & \sigma_w^2/2 \\ 0 & 0 & 0 & \cdots & \cdots & \sigma_w^2/2 & \sigma_w^2 \end{bmatrix}. \tag{5.9}$$

Now we need to find the LR for the three systems.

Binary system

For local binary decision the decision rule at each sensor remains un-changed. For simplicity we use hard decision instead of soft decision detection. The joint probability of the local binary decisions $p(y_1, y_2, \cdots y_N|H_j)$ can be calculated by integration of the the joint pdf of $x_1, x_2, \cdots x_N$ given H_j , which is given by

$$f(x_1, x_2, \cdots x_N|H_j) = \frac{1}{(2\pi)^{N/2}|K_w|^{1/2}} e^{[-\frac{1}{2}(\underline{x}-m)^T K_w^{-1}(\underline{x}-m)]} \tag{5.10}$$

where $\underline{x}$ is the input sequence vector $\{x_i\}_{i=1}^N$. $m = 0$ under H_0 and $m = s$ under H_1. However, the N dimensional integration is not easy to calculate. Instead, we obtained the joint probability of $y_1, y_2, \cdots y_N$ by

$$\begin{aligned} p(y_1, y_2, \cdots y_N|H_j, h_1, \cdots, h_N) &= p(y_1|H_j)p(y_2|H_j, y_1)p(y_3|H_j, y_1, y_2)\cdots p(y_N|H_j, y_1, y_2, \cdots y_{N-1}) \\ &= p(y_1|H_j)p(y_2|H_j, y_1)p(y_3|H_j, y_2)\cdots p(y_N|H_j, y_{N-1}) \\ &= \prod_{i=2}^{N} p(y_i|H_j, y_{i-1})p(y_1|H_j) \\ &= \prod_{i=2}^{N} \frac{p(y_{i-1}, y_i|H_j)}{p(y_{i-1}|H_j)} p(y_1|H_j) \end{aligned}$$

At the fusion center,the received signal is demodulated first and hard decision is applied. The conditional joint probability of $\hat{y}_1, \hat{y}_2, \cdots \hat{y}_N$ is given by

$$\begin{aligned} p(\hat{y}_1, \cdots \hat{y}_N | H_j, h_1, \cdots, h_N) &= \sum_{y_1, \cdots y_N} p(\hat{y}_1, \cdots \hat{y}_N | y_1, \cdots y_N, h_1, \cdots, h_N) p(y_1, \cdots y_N | H_j) \\ &= \sum_{y_1, y_2, \cdots y_N} \prod_{i=1}^{N} p(\hat{y}_i | y_i, h_i) p(y_1, y_2, \cdots y_N | H_j) \end{aligned}$$

Analog system

For analog communication, the received signal at the fusion center is

$$\hat{y}_i = h_i \alpha x_i + n_i$$

The covariance matrix of $\hat{y}_i^N$ can be written as,

$$K_r = \alpha^2 H^T K_r H + I_N \sigma_n^2 \tag{5.11}$$

Where H is the diagonal matrix of the fading gain $\{h_i\}_{i=1}^N$ and $\underline{x}$ is the input vector $\{x_i\}_{i=1}^N$. Since $\{\hat{y}_i\}_{i=1}^N$ is also joint gaussian random vector, we are able to write the joint pdf of $\{\hat{y}_i\}_{i=1}^N$ given $\{h_i\}_{i=1}^N$ and H_j.

$$f(\hat{y}_1, \cdots \hat{y}_N | H_j, h_1, \cdots, h_j) = \frac{1}{(2\pi)^{N/2} |K_r|^{1/2}} e^{[-\frac{1}{2}(\underline{x} - m\underline{h})^T K_r^{-1} (\underline{x} - m\underline{h})]} \tag{5.12}$$

where $\underline{\mathrm{h}}$ is the fading gain vector $\{h_i\}_{i=1}^N$.

$\Sigma - \Delta$ modulation based system

For $\Sigma - \Delta$ ADC, we apply EGC detector since optimal LR based fusion rule is very hard to implement. Our purpose is trying to see if correlation will change the performance discrepancy of $\Sigma - \Delta$ ADC against the other two approaches.

5.2.1 Performance evaluation

Fig. 5.8 gives the detection performance of correlated observations versus N with the covariance matrix of $\{x_i\}_{i=1^N}$ described in (5.9). The performance discrepancy is not substantial

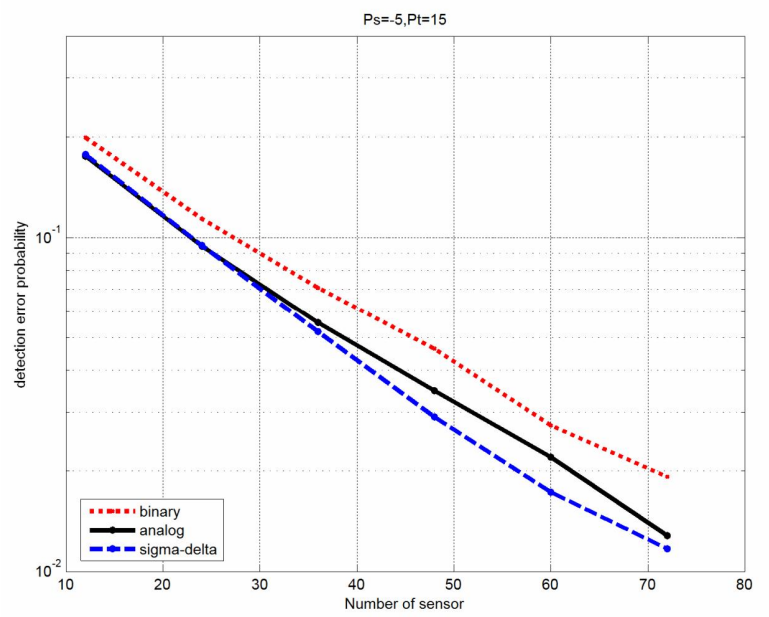

FIGURE 5.9. Detection error probability versus N with correlated observations, P_s=-5dB, P_t=15dB, s=0.5, P_I=15dB, covariance matrix of $\{x_i\}_{i=1^N}$. LRT for analog and binary systems. EGC for $\Sigma-\Delta$ system.

though $\Sigma-\Delta$ modulation based system still outperform the binary and analog system. Recall that in Chapter 2, for single sensor detection using $\Sigma-\Delta$ modulation, we add a feed forward link inside $\Sigma-\Delta$ modulator or add a pre-FIR block to improve the performance. This modification equivalently makes the input from being conditionally independent to correlated. Next we assume the measurement noise covariance matrix is exactly as if we perform a first order filtering to a white input sequence.

The covariance matrix of w_i now becomes

$$K_w = \begin{bmatrix} \sigma_w^2 & \sigma_w^2/2 & 0 & \cdots & \cdots & \cdots & 0 \\ \sigma_w^2/2 & \sigma_w^2/2 & \sigma_w^2/4 & 0 & \cdots & \cdots & 0 \\ 0 & \sigma_w^2/4 & \sigma_w^2/2 & \sigma_w^2/4 & & & \vdots \\ \vdots & \cdots & \cdots & \ddots & \ddots & & \vdots \\ 0 & 0 & \cdots & \cdots & \ddots & \ddots & \vdots \\ 0 & 0 & 0 & \cdots & \cdots & \sigma_w^2/2 & \sigma_w^2/4 \\ 0 & 0 & 0 & \cdots & \cdots & \sigma_w^2/4 & \sigma_w^2/2 \end{bmatrix}. \tag{5.13}$$

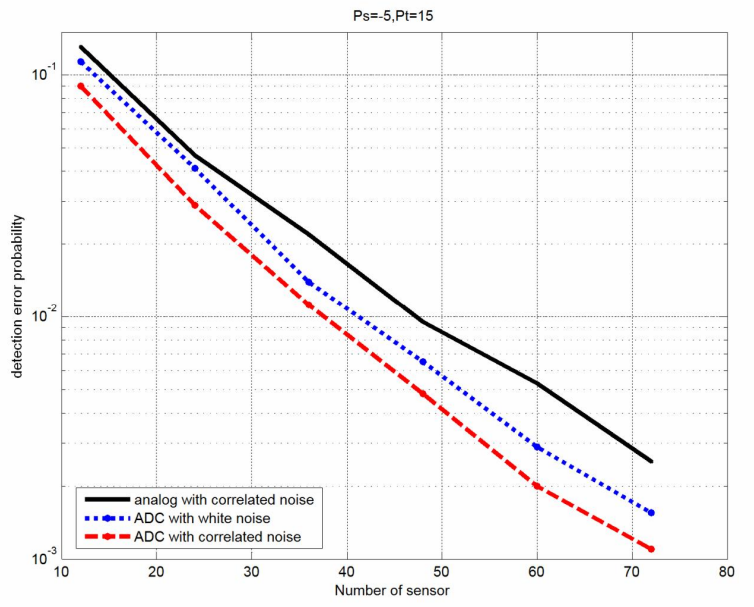

FIGURE 5.10. Detection error probability versus N with correlated observations, P_s=-5dB, P_t=15dB, s=0.5, P_I=15dB, covariance matrix of $\{x_i\}_{i=1^N}$ described in (5.13). LRT for analog and binary systems. EGC for $\Sigma - \Delta$ system.

Applying the optimal fusion rule for analog system obtained in Section 5.2 and EGC for $\Sigma - \Delta$ system, we had another series of simulations as shown in Fig. 5.9. We compare the detection performance of $\Sigma - \Delta$ system to analog system with covariance matrix of $\{x_i\}_{i=1^N}$ described in (5.13), as well as the detection performance of $\Sigma - \Delta$ system with independent observations. It demonstrates that $\Sigma - \Delta$ system has even better performance when observations are not conditionally independent. Although it does not show tremendous superiority against analog system, yet considering binary and analog system uses the optimal coherent detectors that need to obtain channel CSI h_i for every i while $\Sigma - \Delta$ uses suboptimal non-coherent detector that requires minimum channel information, the detection performance for $\Sigma - \Delta$ modulation based system is quite robust.

Summary

In this chapter, we

- Investigate the distributed detection in coherent fading channels and extend the study to detection of correlated observations.
- Provide optimal fusion rule for analog and binary systems in coherent fading channels and of correlated observations.
- Propose another single sensor detection scheme using repetition coding.
- Evaluate the performance of different systems in coherent fading channels and of correlated observations with simulations.

Chapter 6
Conclusion

A novel $\Sigma-\Delta$ modulation based distributed detection scheme is proposed, which essentially transforms the ADC loop from temporal domain to spatial domain. Each sensor does not require global information and only needs to exchange information with its adjacent close neighborhoods. Our simulation result demonstrate this novel mixing of serial and parallel topology can yield better detection performance than the existing schemes under the parallel topology in homogeneous networks (i.e. statistics are all assumed i.i.d here). It reveals that even though we have not optimized the way in exchanging information between adjacent sensors, a simple collaborative processing of observations of sensor nodes outperforms the ones with independent processing.

Our preliminary study thus raises the following fundamental question: what is the optimal way to collaboratively process the local measurements and what is the optimal fusion rule in order to optimize the detection performance under certain constraints imposed by practical issues on the amount of possible collaborations? The $\Sigma - \Delta$ distributed detection scheme should be considered as a special case of such collaborative distributed detection scheme with the constraint that only adjacent sensor nodes are allowed to communicate. Even under such constraint, we can not justify that $\Sigma - \Delta$ is the optimal solution. For example, consider another scheme that each sensor node directly transmits it analog observation to its adjacent sensor and makes a local optimal decision based on two observations (received signal form pervious sensor and its own observation) and transmit the binary decision to the fusion center. Such scheme will certainly yields better performance in high P_t region than $\Sigma-\Delta$ scheme. In addition, we have already shown in chapter 5 that, though maybe hard to implement in distributed detection systems, binary repetition coding scheme has significant

performance improvement by allowing local processing to fully exploit the cooperation of all the local observations. The questions should motivate the future work on optimal collaborative distributed detection while the work presented in this thesis can be considered as a special case under such framework.

References

[1] R. R. Tenney and N. R. S. Jr., "Detection with distributed sensors," *IEEE Trans. Aerosp. Electron. Syst.*, vol. AES-17, no. 4, pp. 501–510, July 1982.

[2] R. Viswanathan and P. K. Varshney, "Distributed detection with multiple sensors: part i: fundamentals," *Proc. IEEE*, vol. 85, no. 1, pp. 54–63, Jan. 1997.

[3] R. S. Blum, S. A. Kassam, and H. V. Poor, "Distributed detection with multiple sensors: part ii: advanced topics," *Proc. IEEE*, vol. 85, no. 1, pp. 64–79, Jan. 1997.

[4] M. D. Srinath, P. K. Rajasekaran, and R. Viswanathan, *Introduction to Statistical Signal Processing with Applications*, 1st ed. Upper Saddle River, NJ: Prentice Hall, 1995.

[5] W. Shi, T. W. Sun, and R. D. Wesel, "Optimal binary distributed detection," in *Proc.IEEE Int. Symp. Inf. Theory*, June 2000, p. 437.

[6] J. F. Chamberland and V. V. Veeravalli, "Decentralized detection in sensor networks," *IEEE Trans. Signal Processing*, vol. 51, no. 2, pp. 407–416, Feb. 2003.

[7] J. Xiao and Z. Luo, "Universal decentralized detection in a bandwidth-constrained sensor network," *IEEE Trans. Signal Processing*, vol. 53, no. 8, pp. 2617–2624, Aug. 2005.

[8] J. Chamberland and V. Veeravalli, "Asymptotic results for decentralized detection in power constrained wireless sensor networks," *IEEE J. Select. Areas Commun.*, vol. 22, no. 6, pp. 1007–1015, Aug. 2004.

[9] B. Chen, L. Tong, and P. K. Varshney, "Channel-aware distributed detection in wireless sensor networks," *IEEE Signal Processing Mag.*, vol. 23, no. 4, pp. 16–26, July 2006.

[10] B. Chen, R. Jiang, T. Kasetkasem, and P. K. Varshney, "Channel aware decision fusion in wireless sensor networks," *IEEE Trans. Signal Processing*, vol. 52, no. 12, pp. 3454–3458, Dec. 2004.

[11] B. Liu and B. Chen, "Decentralized detection in wireless sensor networks with channel fading statistics," in *Proc. 2006 Int. Conf. on Signal Process.*, vol. 4, May 2006, pp. 857–860.

[12] R. Niu, B. Chen, and P. K. Varshney, "Fusion of decisions transmitted over rayleigh fading channels in wireless sensor networks," *IEEE Trans. Signal Processing*, vol. 54, no. 3, pp. 1018–1027, Mar. 2006.

[13] R. S. Blum, "Distributed reception of fading signals in noise," in *Proc. 1995 Int. Symp. on Inform. Theory.*, September 1995, p. 214.

[14] N. S. V. Rao, "Computational complexity issues in synthesis of simple distributed detection networks," *IEEE Trans. Syst., Man, Cybern.*, vol. 21, pp. 1071–1081, Dec. 1991.

[15] P. Willett, P. F. Swaszek, and R. S. Blum, "The good, bad, and ugly: distributed detection of a known signal in dependent gaussian noise," *IEEE Trans. Signal Processing*, vol. 48, no. 12, pp. 469–476, Dec. 2000.

[16] W. Li and H. Dai, "Distributed detection in large-scale sensor networks with correlated sensor observations," in *2005 Allerton Conference on Communication, Control and Computing*, September 2005.

[17] ——, "Distributed detection of a deterministic signal in correlated gaussian noise over mac," in *2006 Int. Symp. on Inform. Theory.*, Seattle, WA, July 2006.

[18] R. S. Blum, "Locally optimum distributed detection of correlated random signals based on ranks," *IEEE Trans. Inform. Theory*, vol. 42, no. 3, pp. 931–942, May 1996.

[19] P. Willett, P. F. Swaszek, and R. S. Blum, "On distributed detection with correlated sensors: two examples," *IEEE Trans. Aerosp. Electron. Syst.*, vol. 25, no. 3, pp. 414–421, May 1989.

[20] G. Bourdopoulos, A. Pnevmatikakis, V. Anastassopolos, and T. L. Deliyannis, *Delta-Sigma Modulators*, 1st ed. River Edge, NJ: Imperial College Press, 2003.

[21] P. M. Aziz, H. V. Sorensen, and J. V. Spiegel, "An overview of sigma-delta converters," *IEEE Signal Processing Mag.*, vol. 13, no. 1, pp. 61–84, Jan. 1996.

[22] A. V. Oppenheim, R. W. Schafer, and J. R. Buck, *Discrete-Time Signal Processing*, 2nd ed. Upper Saddle River, NJ: Prentice Hall, 1999.

[23] T. Koski, "Statistics of the binary quantizer error in single-loop sigma-delta modulation with white gaussian input," *IEEE Trans. Inform. Theory*, vol. 41, no. 4, pp. 931–943, July 1995.

[24] P. W. Wong and R. M. Gray, "Sigma-delta modulation with i.i.d. gaussian inputs," *IEEE Trans. Inform. Theory*, vol. 36, no. 4, pp. 784–798, July 1990.

[25] I. Galton, "Delta-sigma data conversion in wireless trasceivers," *IEEE Trans. Microwave Theory Tech.*, vol. 50, no. 1, pp. 302–315, Jan. 2002.

[26] S. Hoyos, B. Sadler, and G. Arce, "Monobit digital receivers for ultrawideband communications," *IEEE Trans. Wireless Commun.*, vol. 4, no. 4, pp. 1337–1344, July 2005.

[27] K. Opasjumruskit, "Self-powered wireless temperature sensors exploit rfid technology," *IEEE Pervasive Computing*, pp. 54–61, Jan. 2006.

[28] J. G. Proakis, *Digital Communications*, 4th ed. New York: McGraw- Hill, 2001.

[29] A. Goldsmith, *Wireless Communications*, 1st ed. New York: Cambridge University Press, 2005.

Appendix: Matlab code of optimal fusion algorithm for $\Sigma - \Delta$ modulation based distributed detection system

```
%    Optimal non-coherent detection algorithm for Sigma-Delta ADC
%    based distributed detection system over Rayleigh fading channel.
%    The fusion center makes a global decision $\theta$ regarding
%    the hypothesis H_j upon receiving {yhat(1),yhat(2),...,yhat(N)}
%    based on LRT rule.
%
%
%    Number of sensors $N$, sensoring SNR $P_s$, channel SNR $P_t$,
%    inter-sensor channel SNR $P_I$, constant $s$ in the input signal
%    under H_1 need to specified prior to running the algorithm.
%^   Channel CSI is not required for this algorithm.
%    The performance of this detection algorithm depends on the resolution
%    of the numerical convolution, which can be modified correspondingly.
%
%
%
%     Copyright Dimeng Wang, LSU
%     Date: 2007/03/09 16:16:08
%


%- Calculate $\sigma_w$, $\sigma_n$, $\sigma_{\eta}$
sigma_w=sqrt((s^2/((10^(0.1*P_s))*2)));
```

```
sigma_n=sqrt(((1)/((10^(0.1*P_t))*2)));
sigma_eta=sqrt(((1)/((10^(0.1*P_I))*2)));


%- Calculate the joint pdf of {yhat(1),...,yhat(N)} conditional on H_1
%- First get the numerical pdf of x, eta, and v_1
m=s;
x=[-2:0.005:3];
pr=exp(-((x-m).*(x-m))/(2*sigma_w^2))/(sqrt(2*pi*sigma_w^2));
pr=pr/(sum(pr));
x=[-1:0.005:1];
peta=exp(-((x).*(x))/(2*sigma_I^2))/(sqrt(2*pi*sigma_I^2));
peta=peta/sum(peta);
x=[-3:0.005:4];
pv=exp(-((x-m).*(x-m))/(2*sigma_w^2))/(sqrt(2*pi*sigma_w^2));
pv=pv/(sum(pv));

%- Get the probability of y_1 given yhat_1
y=yhat(1);
a=1/(sigma_n*(sqrt(1+2*sigma_n^2)));
py_1=2*sigma_n/(sqrt(2*pi)*(1+2*sigma_n^2))*exp(-y^2/(2*sigma_n^2))
*(1+sqrt(2*pi)*a*y*exp((a*y)^2/2)*qfunc(-a*y));
py_0=2*sigma_n/(sqrt(2*pi)*(1+2*sigma_n^2))*exp(-y^2/(2*sigma_n^2))
*(1+sqrt(2*pi)*a*-y*exp((a*y)^2/2)*qfunc(a*y));
summ_y=py_1+py_0;
py_1=py_1/summ_y;
```

```
py_0=py_0/summ_y;

%- Get the pdf of yhat_1
pyh(1)=((sum(pv(602:1401))+pv(601)/2))/sum(pv)*py_1+
((sum(pv(1:600))+1/2*pv(601)))/sum(pv)*py_0;



for n=1:(N-1);

    %- Get the probability of y_n given yhat_n
    y=yhat(n);
    py1(n)=2*sigma_n/(sqrt(2*pi)*(1+2*sigma_n^2))*exp(-y^2/(2*sigma_n^2))
    *(1+sqrt(2*pi)*a*y*exp((a*y)^2/2)*qfunc(-a*y));
    py0(n)=2*sigma_n/(sqrt(2*pi)*(1+2*sigma_n^2))*exp(-y^2/(2*sigma_n^2))
    *(1+sqrt(2*pi)*a*-y*exp((a*y)^2/2)*qfunc(a*y));
    summ_y=py1(n)+py0(n);
    py1(n)=py1(n)/summ_y;
    py0(n)=py0(n)/summ_y;

    %- Get the pdf of v_n given y_n and yhat_n
    pv_y1=pv;
    pv_y0=pv;
    pv_y1(1:600)=0;
    pv_y1(601)=pv_y1(601)/2;
    pv_y1=pv_y1/sum(pv_y1);
    pv_y0(602:1401)=0;
```

```
pv_y0(601)=pv_y0(601)/2;
pv_y0=pv_y0/sum(pv_y0);

%- Get the pdf of v_n given yhat_n
pv=py1(n)*(pv_y1)+py0(n)*(pv_y0);
pv=pv/sum(pv);

% Get the pdf of \tilde{v}_n given yhat_n
pv=conv(pv,peta);
pv=pv(201:1601);
pv=pv/sum(pv);

% Get the pdf of e_n given yhat_n
pe(201:601)=pv(601:1001)+pv(201:601);
pe(1:200)=pv(1:200);
pe(601:1001)=pv(1001:1401);
pe=pe/sum(pe);

% Get the pdf of v_{n+1} and the probability of y_{n+1} given yhat_n
pv=conv(pr,pe);
pv=pv/sum(pv);
py1t(n+1)=sum(pv(802:2001))+1/2*pv(801);
py0t(n+1)=sum(pv(1:801))+1/2*pv(802);
pv=pv(201:1601);
pv=pv/sum(pv);
y=yhat(n+1);
```

```
    py_1=2*sigma_n/(sqrt(2*pi)*(1+2*sigma_n^2))*exp(-y^2/(2*sigma_n^2))
    *(1+sqrt(2*pi)*a*y*exp((a*y)^2/2)*qfunc(-a*y));
    py_0=2*sigma_n/(sqrt(2*pi)*(1+2*sigma_n^2))*exp(-y^2/(2*sigma_n^2))
    *(1+sqrt(2*pi)*a*-y*exp((a*y)^2/2)*qfunc(a*y));

    %- Get the pdf of yhat_{n+1} given yhat_n
    pyh(n+1)=py1t(n+1)*py_1+py0t(n+1)*py_0;
end

%- Get the joint pdf of {yhat(1),...,yhat(N)} conditional on H_1
pyh_H1=prod(pyh);

%- Repeat the procedure for the joint pdf of {yhat(1),...,yhat(N)}
%conditional on H_0

m=0;
x=[-2:0.005:3];
pr=exp(-((x-m).*(x-m))/(2*sigma_w^2))/(sqrt(2*pi*sigma_w^2));
pr=pr/(mean(pr)*length(pr));
x=[-3:0.005:4];
pv=exp(-((x-m).*(x-m))/(2*sigma_w^2))/(sqrt(2*pi*sigma_w^2));
pv=pv/(sum(pv));
x=[-1:0.005:1];
peta=exp(-((x).*(x))/(2*sigma_I^2))/(sqrt(2*pi*sigma_I^2));
peta=peta/sum(peta);
```

```
y=yhat(1);
py_1=2*sigma_n/(sqrt(2*pi)*(1+2*sigma_n^2))*exp(-y^2/(2*sigma_n^2))
*(1+sqrt(2*pi)*a*y*exp((a*y)^2/2)*qfunc(-a*y));
py_0=2*sigma_n/(sqrt(2*pi)*(1+2*sigma_n^2))*exp(-y^2/(2*sigma_n^2))
*(1+sqrt(2*pi)*a*-y*exp((a*y)^2/2)*qfunc(a*y));
pyh(1)=((sum(pv(602:1401))+pv(601)/2))/sum(pv)*py_1+
(sum(pv(1:600))+1/2*pv(601))/sum(pv)*py_0;
summ_y=py_1+py_0;
py_1=py_1/summ_y;
py_0=py_0/summ_y;

for n=1:(N-1);
    y=yhat(n);
    py1(n)=2*sigma_n/(sqrt(2*pi)*(1+2*sigma_n^2))*exp(-y^2/(2*sigma_n^2))
    *(1+sqrt(2*pi)*a*y*exp((a*y)^2/2)*qfunc(-a*y));
    py0(n)=2*sigma_n/(sqrt(2*pi)*(1+2*sigma_n^2))*exp(-y^2/(2*sigma_n^2))
    *(1+sqrt(2*pi)*a*-y*exp((a*y)^2/2)*qfunc(a*y));
    summ_y=py1(n)+py0(n);
    py1(n)=py1(n)/summ_y;
    py0(n)=py0(n)/summ_y;
    pv_y1=pv;
    pv_y0=pv;
    pv_y1(1:600)=0;
    pv_y1(601)=pv_y1(601)/2;
    pv_y1=pv_y1/sum(pv_y1);
```

```
    pv_y0(602:1401)=0;
    pv_y0(601)=pv_y0(601)/2;
    pv_y0=pv_y0/sum(pv_y0);
    pv=py1(n)*(pv_y1)+py0(n)*(pv_y0);
    pv=pv/sum(pv);
    pv=conv(pv,peta);
    pv=pv(201:1601);
    pv=pv/sum(pv);
    pe(201:601)=pv(601:1001)+pv(201:601);
    pe(1:200)=pv(1:200);
    pe(601:1001)=pv(1001:1401);
    pe=pe/sum(pe);
    pv=conv(pr,pe);
    pv=pv/sum(pv);
    py1t(n+1)=sum(pv(802:2001))+1/2*pv(801);
    py0t(n+1)=sum(pv(1:801))+1/2*pv(802);
    pv=pv(201:1601);
    pv=pv/sum(pv);
    y=yhat(n+1);
    py_1=2*sigma_n/(sqrt(2*pi)*(1+2*sigma_n^2))*exp(-y^2/(2*sigma_n^2))
    *(1+sqrt(2*pi)*a*y*exp((a*y)^2/2)*qfunc(-a*y));
    py_0=2*sigma_n/(sqrt(2*pi)*(1+2*sigma_n^2))*exp(-y^2/(2*sigma_n^2))
    *(1+sqrt(2*pi)*a*-y*exp((a*y)^2/2)*qfunc(a*y));
    pyh(n+1)=py1t(n+1)*py_1+py0t(n+1)*py_0;
end
```

```
pyh_H0=prod(pyh);


%- Compute the likelihood ratio of {yhat(1),...,yhat(N)}
%- and make the global decision based on the LRT fusion rule.


if pyh_H1/pyh_H0>1;
   theta=1;
else
   theta=-1;
end
```

Vita

Dimeng Wang was born on Aug 26th 1983, in Shanghai, China. He finished his undergraduate studies at Electrical Engineering Department, Shanghai Jiaotong University, China, in June 2005. In August 2005, he came to Louisiana State University to pursue graduate studies in wireless communications. He is currently a candidate for the degree of Master of Science in Electrical Engineering, which will be awarded in August 2007.